ETC-based control of underactuated AUVs and AUV formations in a 2D plane

Master 's Thesis

Facultat de Nàutica de Barcelona
Universitat Politècnica de Catalunya

Work done by:
Jiaqi. Yao

Directed by:
Sergio Romero
Rosa M. Fernández

Master in Naval Architecture and Ocean Engineering

Barcelona, May, 2022

Facultat de Nàutica de Barcelona.

Version	Data	Modifications
1	10/02/2022	Document creation
2	14/03/2022	Format and content modifications
3	10/05/2022	Format modifications and Content supplement

Written by:	
Author:	Jiaqi. Yao
Date:	10/02/2022

Revised and approved by:	
Tutor:	Sergio Romero
Date:	16/02/2022
Revised and approved by:	
Co-Tutor:	Rosa M. Fernández
Date:	27/02/2022

Written by:	
Author:	Jiaqi. Yao
Date:	14/03/2022

Revised and approved by:	
Tutor:	Sergio Romero
Date:	23/03/2022
Revised and approved by:	
Co-Tutor:	Rosa M. Fernández
Date:	28/03/2022

Written by:	
Author:	Jiaqi. Yao
Date:	10/05/2022

Revised and approved by:	
Tutor:	Sergio Romero
Date:	26/05/2022
Revised and approved by:	
Co-Tutor:	Rosa M. Fernández
Date:	

Acknowledgments

The master thesis was completed much later than planned for various reasons. But many of my friends, teachers and classmates gave me a lot of help and encouragement during my difficult times.

Now, finally I finish it. I would like to thank my tutor Professor Romero, Professor Fernández, Professor Li Jiawang as well as Professor Wang Yuhong, who helped me to continue my studies at UPC during this time.

Thanks also to UPC and NBU for giving me an unforgettable study abroad experience and giving me the opportunity to finish this thesis after I delayed so long.

Abstract

This master thesis is aimed at single AUV (Autonomous Underwater Vehicle) and AUV formation control in two-dimensional horizontal plane. For sake of increasing services life and saving communication resources, Event-triggered mechanism is taken into consideration.

Two coordinate systems are introduced: Earth-fixed frame and body-fixed frame. Some motion parameters and force analysis are used in the process of establishing mathematical model.

Then the related theorems, lemmas and control method commonly used in analyzing control systems are introduced.

Then, the AUV control system is divided into two subsystems with cascade relationship. Considering each subsystem separately, a controller is designed that can simultaneously carry out trajectory tracking and point stabilization.

Considering the service life of actuator equipment, an event-triggered controller was designed, which can reduce the frequency of actuator adjustment, prolong the service life of equipment.

Finally, combining the idea of Light-of-sight method and virtual structure method, the AUV formation tracking control problem is solved similarly to single AUV.

In deep sea conditions, an Event- triggered communicating mechanism is designed to reduce the frequency of communication and adapt to limited communication resources, which balances the reliability and economy.

MATLAB Simulink is used to simulate the controller designed in the thesis, and confirms the feasibility of the controller.

Keywords: “Underactuated AUV”, “Event-triggered Control”, “AUV Formation”

Table of contents

List of Figures

List of Tables

Chapter 1. Introduction

With the continuous development of modern technology, human beings have become increasingly cautious about exploiting the limited resources on land.

The ocean accounts for about 71% of the Earth's surface area and is rich in natural gas, oil, biological and mineral resources. It also has non-fossil energy sources such as tidal power, wind power and temperature difference energy, which makes human beings turn their attention to the ocean instead of land. In ocean research, the deep sea below 1000m has not been fully exploited and is the hot spot for resource development in the future.

Due to the limitation of physiological conditions, it is difficult for human beings to conquer and utilize the ocean by themselves. They must use underwater equipment. Underwater vehicles can assist or replace human beings to complete underwater mapping, detection and operations by remote control or autonomous operation.

Underwater vehicles are divided into MUV (Manned Underwater vehicle) and UUV (Unmanned Underwater vehicle) according to whether they can carry people. The latter can be divided into ROV (Remotely Operated Vehicle) and AUV (Autonomous Underwater Vehicle) based on the form of motion and control.

Figure 1. ROV [15]

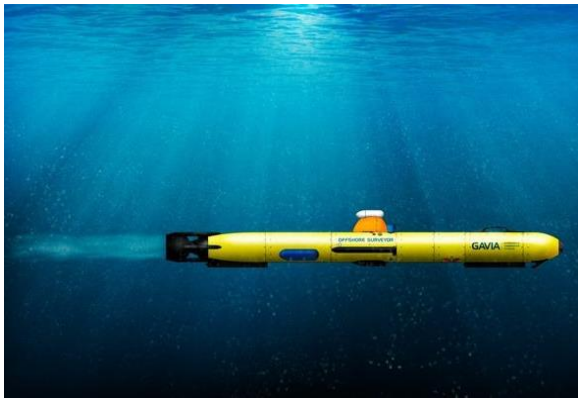

Figure 2. AUV [16]

Autonomous underwater vehicles (AUV) are very suitable tools for seabed search, ocean mapping, salvage and other operations, but also can be used as military equipment, for underwater mine clearance, reconnaissance, surveillance, carrying mine heads to the target sea area, serve as a target, and other works, both economic and security.

AUV are mainly composed of sensor system, communication positioning system, electric control system, power propulsion system and so on. Compared with MUV, AUV do not need to carry a person, so it is safe, light, small, simple and low cost. Compared to ROVs, AUVs are wireless, giving them a wide range of activities, deep dives, access to complex structures without cable entanglement, and no need for large surface support or deck areas. Therefore, AUVs represent the development direction of future underwater robot technology and is a hotspot of current research and development.

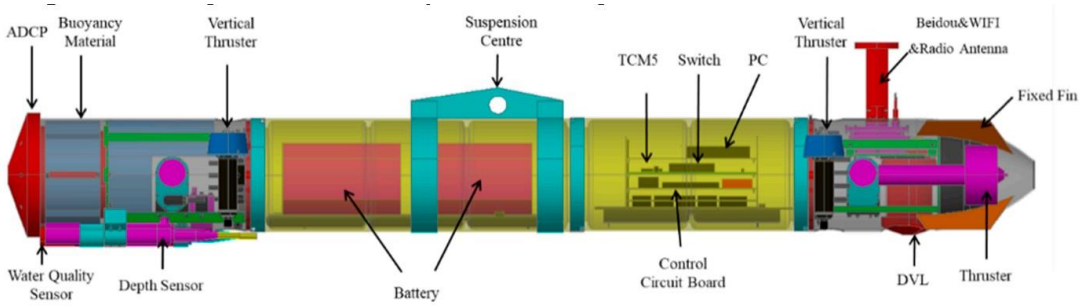

Figure 3. Structure of AUV[17]

As ocean exploration continues to deepen, more complex missions put higher demands on AUV performance. In the face of tasks with larger scope and higher timeliness requirements, it is difficult to complete them only by relying on a single AUV.

Multiple Autonomous Underwater Vehicle System (MAUVS) refers to a system composed of multiple AUV, where the individuals in the system can exchange their respective state information, the sensor data and control information. They coordinate with each other and form a whole, carrying out efficient data collection and complete specific tasks.

In recent years, after repeated system design and experiments, MAUVSs have developed the ability to carry out continuous operations in complex Marine environments and become an efficient and reliable underwater observation system. MAUVSs collaborative motion has the advantages of strong adaptability, high fault tolerance, high operating efficiency and wide operating range.

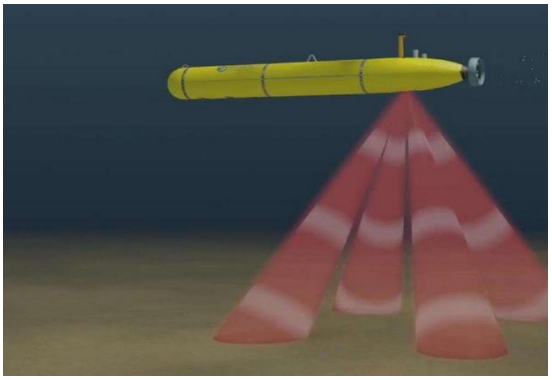

Figure 4. A single AUV performing tasks [18]

Figure 5. AUV formation [19]

For AUVs, how to control their motion effectively in the complex deep-sea environment is a very basic and important problem.

According to its control objectives, the motion control of the underactuated AUV can be divided into stabilization control, trajectory tracking control, path tracking control and multi-AUV formation control

Stabilization control was first proposed by Samson in 1995 (Samson, 2002), which means that under the continuous excitation of control input, underactuated AUV with the initial state of arbitrary position and attitude reaches the specified target point and remains stable.

Trajectory tracking control means that AUV starts from any given initial state and arrives at and follows the desired route, which has time and space requirements and needs to arrive at the corresponding position at a specified time.

Path tracking control means that AUV starts from any given initial state, arrives at a given velocity and follows the desired geometric path, which is independent of time variable and AUV only needs to meet the specified space position (Lapierre & Jouvencel, 2007).

The control research of AUV mainly has the following difficulties:

(1) The underactuation of AUV, that is, AUV is a non-holonomic constrained system: the number of controlled outputs is greater than the number of control inputs;

(2) Coupling of AUV: AUV with six degrees of freedom in three-dimensional space, three translational motion (surging, swaying and heaving, usually controlled by the propeller of each direction) and three rotations (rolling, pitching, and yawing, usually control by each direction rudder). The movement of the actuator of each operation will also affect other direction of movement, which leads to the coupling between the various degrees of freedom;

(3) External interference and model uncertainty: The working environment of AUV is complex, which is affected by various environmental factors such as wave, temperature, water pressure and ocean current. Such interference usually changes with time, which increases the difficulty of AUV modeling;

(4) Nonlinear control model: AUV model parameters are different with different motion states. For example, hydrodynamic coefficient will change with velocity, leading to nonlinear characteristics of the whole system.

Multi-AUV formation control refers to the formation of a complex system among multiple AUVs through mutual communication. Individuals can perceive changes in the external environment, communicate with each other, and make collective behaviors to achieve a unified goal.

Multi-AUV formation control problem is a typical problem of multi-agent cooperative control, which means that multiple AUVs maintain the desired formation through control input under the condition of adapting to environmental constraints in the process of reaching the destination or tracking task.

When multi-AUV formation performs tasks, it is necessary to exchange information with other AUVs through network topology, so as to coordinate within the formation to complete complex tasks. However, in the actual underwater work process, the computing power and communication resources of AUVs are often very limited. Communication between AUVs in formation is often limited, so real-time communication cannot be carried out, and the controller inside a single AUV cannot be updated in real time.

For this kind of problem, the traditional solution is to adopt the time-trigger mechanism, which sets the trigger time in advance without considering the state of the system in operation. This method can reduce the frequency of the formation's communication and calculation to a certain extent, and reduce the cost.

However, there are the following problems: first, when AUV is in the process of approaching convergence, or the interference is small, the change of system state is very slow. In this case, the use of time trigger will lead to resource waste; secondly, to ensure the reliability of

time trigger, too long trigger period should not be set, but a small trigger period will lead to high sampling frequency, and there is still the problem of too much redundant information, which increases the burden of network sensors and AUV internal computing hosts, and cannot significantly reduce the cost.

In order to balance reliability and economy, many researchers turn their attention to event-trigger control (ETC).

Event triggering means that a triggering condition is set in advance before AUV enters work. If the control condition meets the triggering condition during work, the system determines that an event has occurred and performs the triggering task to transfer information between AUVs in the team or update the internal control input of AUVS. The triggering condition is usually set as: the state error of the system exceeds a certain threshold, which is usually related to the state or time of the system (Yu, Xia, Li, & Zhai, 2020).

Compared with time trigger, the sampling time of event trigger depends on whether the system state meets the trigger condition. Therefore, the sampling time is more flexible, which can effectively reduce the execution times of power actuator and communication times of communication equipment. Therefore, the hardware loss is reduced, the communication and computing resources is saved, and costs saved, too.

This thesis mainly discusses the underactuated AUV individual and formation control problem. The main content of the paper is divided into six chapters, Firstly, Chapter 1 describes the interest of deep-sea field technology development, and the importance of AUV to the development of deep-sea engineering. Then it briefly describes the composition of AUV and the concept of AUV formation. Finally, the control difficulties of single AUV and multi-AUV formation and the event triggering mechanism are introduced respectively.

Chapter 2 describes the research objectives and outlines the scope of this study.

Chapter 3 introduces the AUV model, the theoretical basis of AUV control and some simple graph theory.

In Chapter 4, controller design, improvement and simulation analysis are carried out for stabilization control and trajectory tracking control tasks of a single AUV.

In Chapter 5, controller design, formation communication strategy design and simulation analysis are carried out for multi-AUV formation trajectory tracking task.

Chapter 6 summarizes the research work of the whole thesis and puts forward some suggestions for future improvement.

Chapter 2. Objective

2.1. Objectives

The main objective of this work is to design appropriate control strategy for a single AUV and multi-AUV formation respectively to make them perform stabilization or trajectory tracking tasks.

To obtain the objective it is necessary to point all the steps and tasks required to develop it. These secondary objectives are set as follows:

• Collect and organize the theoretical basis of AUV control.

• Identify kinematic and dynamic models of AUV.

• Design a controller for a single AUV, then use Simulink to test it.

• Design a mechanism to optimize the controller, use Simulink to check the performance.

• Design a following rule for multi-AUV formation, then use Simulink to assess the performance.

• Summarize the research work of the whole thesis and put forward some suggestions for future improvement.

2.2. Project timeline

No.	TASK	START TIME	DURATION
1	Collect and classify reference materials	2021/4/1	15 days
2	Learn about the theoretical basis of AUV control	2021/4/10	20 days
3	Identify kinematic and dynamic models of AUV	2021/5/1	10 days
4	Controller design and prove theoretically for single AUV	2021/5/10	15 days

5	Simulation for single AUV control	2021/5/15	5 days
6	Optimize the controller	2021/5/20	20 days
7	Following rule design and prove theoretically for AUV formation	2021/6/10	15 days
8	Simulation for single AUV formation control	2021/6/25	5 days
9	Optimize the following rule	2021/7/1	20 days
10	Write the thesis	2021/7/20	30 days
11	Improve the thesis	2022/2/10	20 days

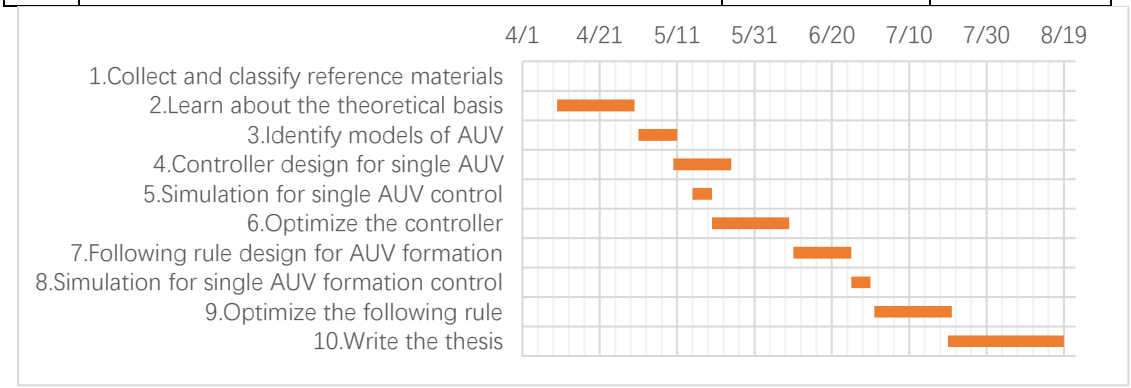

Table 1. Project timeline

Chapter 3. Theoretical Background

In order to complete this thesis, it is necessary to understand the theoretical basis of AUV control.

Chapter 3 is mainly divided into six sections, which elaborate the working principle of the project from the perspective of theory.

The selection of appropriate control model is the basis of control design. AUV is a very typical nonholonomic nonlinear model, and the interference brought by the work environment and the influence factors of uncertainty is also complex. Using an accurate model of a real AUV makes the controller design process very complicated and difficult to implement. Therefore, it is necessary to simplify the model and choose a model with appropriate accuracy and widely accepted by the academic community.

In section 3.1, based on the motion characteristics and force on underactuated AUV, standard definitions of earth-fixed coordinate frame and body-fixed coordinate frame are made, and relevant parameters of each coordinate system are explained.

Section 3.2 introduces the transformation between two coordinate systems, and gives the kinematics model of AUV according to the transformation matrix. According to the analysis of the external force of AUV under water, the dynamic model of AUV was established, with the explanation of the physical meaning of each matrix. In order to facilitate the subsequent control design, the above dynamics and kinematics models were simplified, and the two-dimensional plane kinematics equations and dynamics equations of AUV motion were obtained.

Section 3.3 introduces several common motion control methods of AUV, and analyzes their advantages and disadvantages.

Section 3.4 introduces Lyapunov stability and other related theories, which is convenient for analysis in subsequent chapters.

Section 3.5 introduces several commonly used multi-AUV formation control methods and analyzes their advantages and disadvantages.

Section 3.6 introduces several formation strategies for AUVs and explains the strategies chosen for this paper.

All the contents of the document that are not your own must be duly referenced. Failure to do so may be considered plagiarism.

3.1. Coordinate system and motion parameters

In order to describe the motion state of AUV accurately, it is necessary to select an appropriate coordinate system as a reference.

In this thesis, the motion of AUV will be described by using the general coordinate system definition published by ITTC (International Towing Tank Conference) and SNAME (Society of Naval Architects and Marine Engineers).(SNAME,1950)

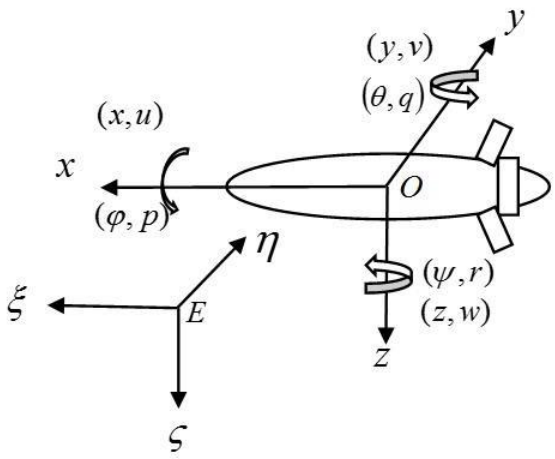

Figure 6. Earth-fixed and body-fixed coordinate frames [20]

Earth-fixed frame ($E-\xi\eta\zeta$) is the inertial reference frame of AUV motion, which is used to describe the space position and attitude angle of AUV motion. The origin E, can be selected as any point on the sea or in the sea, or the position of AUV motion at time zero. The axis $E\xi$ is located in the horizontal plane, pointing to any specified direction; The axis $E\eta$ is also located in the horizontal plane, perpendicular to $E\xi$, which can be obtained by rotating $E\eta$ 90° clockwise according to the right-hand rule. $E\zeta$ satisfies the right-hand rule, perpendicular to the coordinate plane $E-\xi\eta$,and pointing toward the center of the earth.

The body-fixed frame ($O-xyz$), moves along with AUV, and the origin O is generally taken as the center of gravity or buoyance center of AUV. The axis Ox is parallel to the water surface and points to bow. The axis Oy is perpendicular to the axis Ox and points to starboard. Axis Oz is perpendicular to the coordinate plane $O-xy$ and points to the bottom of the boat, satisfying the right-hand rule. When the origin O of the body-fixed frame is located at the barycenter (center of gravity) position, Ox, Oy and Oz are considered to be the inertia principal axes of AUV.

The translation of AUV in the x direction is called the surge, the translation in the y direction is called the sway, and the translation in the z direction is called the heave. The rotation along the x axis is called roll and the corresponding rotation angle is roll angle φ; the rotation along the y axis is called pitch and the corresponding rotation angle is pitch angle θ; the rotation along the z direction is called yaw and the corresponding rotation angle is yaw angle ψ.

The vector $\boldsymbol{\eta}_1=(x,y,z)^T$ is defined as the global space position coordinate in the earth-fixed frame of the origin of body-fixed frame, and the rotation vector $\boldsymbol{\eta}_2=(\varphi,\theta,\psi)^T$ is the attitude angle of the AUV's body-fixed frame relative to the earth-fixed frame.

The projection of AUV's velocity relative to the earth on the body-fixed frame $O-xyz$ is longitudinal velocity u, transverse velocity v and vertical velocity w. The projection of AUV's rotational angular velocity on the body-fixed frame is roll velocity p, pitch velocity q and yaw velocity r.

The velocity vector $\boldsymbol{v}_1=(u,v,w)^T$ is defined as the linear velocity of AUV along the three coordinate axes of the body-fixed frame, and $\boldsymbol{v}_2=(p,q,r)^T$ as the angular velocity of AUV along the three axes of the body-fixed frame.

The projection components of the external force on AUV in the body-fixed frame $O-xyz$ are longitudinal force X, transverse force Y and vertical force Z. The external moments

subjected to AUV are the roll moment K along the axis x, pitch moment M along the axis y, and yaw moment N along the axis z respectively.

Motion parameters	Axis ξ	Axis η	Axis ζ
Displacement	x	y	z
Angle	φ	θ	ψ

Table 2. Motion parameters in the earth-fixed frame

Motion parameters	Axis x	Axis y	Axis z
Velocity	u	v	w
Angular velocity	p	q	r
External force	X	Y	Z
Moment	K	M	N

Table 3. The motion parameters and the projected components of the forces in the body-fixed frame

3.2. Mathematical model of underactuated AUV

3.2.1. Kinematic model of underactuated AUV

When AUV is working, the velocity and angular velocity signals measured by the sensor mounted on AUV usually take the body-fixed frame as the reference system. However, AUV motion is usually analyzed in earth-fixed frame during controller design. Generally, the direction of origin and coordinate axes of the two are not consistent. In order to facilitate the analysis of the kinematic characteristics of AUV, it is necessary to convert variables in the earth-fixed frame $E-\xi\eta\zeta$ and the body-fixed frame$O-xyz$.

The relative relationship between the earth-fixed frame and the body-fixed frame can be expressed by translation and rotation. The translation can be expressed by the coordinates of the origin of the body-fixed frame in the earth-fixed frame, while rotation is generally used three times to make the earth-fixed frame coincide with the body-fixed frame in each axis.

(1)Firstly, rotate the yaw angle ψ about the axis $E\zeta$： $E\xi \to Ex_1$， $E\eta \to Ey_1$；

(2)Then rotate the pitch angle θ about the axis Ey_1： $Ex_1 \to Ex$， $E\zeta \to Ez_1$；

(3)Finally, rotate the roll angle φ about the axis Ex： $Ey_1 \to Ey$， $Ez_1 \to Ez$；

The angles of these three rotations are called Euler angles, which uniquely determine the orientation (attitude) of the AUV in space.

The transformation of the above coordinate system can be expressed as a matrix transformation:

$$\begin{bmatrix} \xi \\ \eta \\ \zeta \end{bmatrix} = \boldsymbol{J}_1(\boldsymbol{\eta}_2) \begin{bmatrix} x \\ y \\ z \end{bmatrix} \tag{1}$$

Among them, $J_1(\eta_2)$ is used to represent the transformation process:

$$\boldsymbol{J}_1(\boldsymbol{\eta}_2) = \boldsymbol{H}_{z,\psi}\boldsymbol{H}_{y,\theta}\boldsymbol{H}_{x,\varphi} \tag{2}$$

Matrix $\boldsymbol{H}_{z,\psi}$, $\boldsymbol{H}_{y,\theta}$, $\boldsymbol{H}_{x,\varphi}$ represent transformation steps (1), (2) and (3) respectively:

$$\boldsymbol{H}_{z,\psi} = \begin{bmatrix} \cos\psi & -\sin\psi & 0 \\ \sin\psi & \cos\psi & 0 \\ 0 & 0 & 1 \end{bmatrix}, \boldsymbol{H}_{y,\theta} = \begin{bmatrix} \cos\theta & 0 & \sin\theta \\ 0 & 1 & 0 \\ -\sin\theta & 0 & \cos\theta \end{bmatrix}, \boldsymbol{H}_{x,\varphi} = \begin{bmatrix} 1 & 0 & 0 \\ 0 & \cos\varphi & -\sin\varphi \\ 0 & \sin\varphi & \cos\varphi \end{bmatrix} \tag{3}$$

By substituting (3) into (2), a complete coordinate transformation matrix can be obtained:

$$\boldsymbol{J}_1(\boldsymbol{\eta}_2) = \begin{bmatrix} \cos\psi\cos\theta & \cos\psi\sin\varphi\sin\theta - \sin\psi\cos\varphi & \cos\psi\sin\theta\cos\varphi + \sin\psi\sin\varphi \\ \sin\psi\cos\theta & \sin\psi\sin\theta\sin\varphi - \cos\psi\cos\varphi & \sin\psi\sin\theta\cos\varphi - \cos\psi\sin\varphi \\ -\sin\theta & \cos\theta\sin\varphi & \cos\theta\cos\varphi \end{bmatrix} \tag{4}$$

According to the previous section, in the earth-fixed frame, the linear velocity of the underactuated AUV is $\dot{\boldsymbol{\eta}}_1 = (\dot{x},\dot{y},\dot{z})^T$;the angular velocity is $\dot{\boldsymbol{\eta}}_2 = \left(\dot{\varphi},\dot{\theta},\dot{\psi}\right)^T$. In the body-fixed frame, the linear velocity is $\boldsymbol{v}_1 = (u,v,r)^T$,the angular velocity is $\boldsymbol{v}_2 = (p,q,r)^T$. Then the

transformation relation of linear velocity and angular velocity between earth-fixed frame and body-fixed frame is:

$$\begin{cases} \dot{\boldsymbol{\eta}}_1 = \boldsymbol{J}_1(\boldsymbol{\eta}_2)\boldsymbol{v}_1 \\ \dot{\boldsymbol{\eta}}_2 = \boldsymbol{J}_2(\boldsymbol{\eta}_2)\boldsymbol{v}_2 \end{cases} \tag{5}$$

where $\boldsymbol{J}_1(\boldsymbol{\eta}_2)$ is called the linear velocity transformation matrix, as described in the previous section; $\boldsymbol{J}_2(\boldsymbol{\eta}_2)$ is called angular velocity transformation matrix, and its expansion formula is:

$$\boldsymbol{J}_2(\boldsymbol{\eta}_2) = \begin{bmatrix} 1 & \sin\varphi\tan\theta & \cos\varphi\tan\theta \\ 0 & \cos\varphi & -\sin\varphi \\ 0 & \sin\varphi/\cos\theta & \cos\varphi/\cos\theta \end{bmatrix} \tag{6}$$

According to the equation (4), (5) and (6), the 6-DOF kinematic model of underactuated AUV is:

$$\begin{cases} \dot{x} = u\cos\psi\cos\theta + v(\cos\psi\sin\theta\sin\varphi - \sin\psi\cos\varphi) + w(\cos\psi\sin\theta\cos\varphi + \sin\psi\sin\theta) \\ \dot{y} = u\sin\psi\cos\theta + v(\sin\psi\sin\theta\sin\varphi + \cos\psi\cos\varphi) + w(\sin\psi\sin\theta\cos\varphi - \cos\psi\sin\varphi) \\ \dot{z} = -u\sin\theta + v\cos\theta\sin\varphi + w\cos\theta\cos\varphi \\ \dot{\varphi} = p + q\sin\varphi\tan\theta + r\cos\varphi\tan\theta \\ \dot{\theta} = q\cos\varphi - r\sin\varphi \\ \dot{\psi} = q\sin\varphi/\cos\theta + r\cos\varphi/\cos\theta \end{cases} \tag{7}$$

It can be expressed in matrix form as:

$$\dot{\boldsymbol{\eta}} = \boldsymbol{J}(\boldsymbol{\eta})\boldsymbol{v} \tag{8}$$

namely:

$$\begin{bmatrix} \dot{\boldsymbol{\eta}}_1 \\ \dot{\boldsymbol{\eta}}_2 \end{bmatrix} = \begin{bmatrix} \boldsymbol{J}_1(\boldsymbol{\eta}_2) & \boldsymbol{O}_{3\times3} \\ \boldsymbol{O}_{3\times3} & \boldsymbol{J}_2(\boldsymbol{\eta}_2) \end{bmatrix} \begin{bmatrix} \boldsymbol{v}_1 \\ \boldsymbol{v}_2 \end{bmatrix} \tag{9}$$

It should be noted that when $\theta = \pm 90^\circ$, the transformation matrix is meaningless. At this time, $\boldsymbol{J}_2(\boldsymbol{\eta}_2) \neq \boldsymbol{J}_2^T(\boldsymbol{\eta}_2)$.

3.2.2. Dynamic model of underactuated AUV

When studying the motion control of AUV, AUV is usually considered as a rigid body.

In the ocean, the external forces on the AUV is: static force (including gravity and buoyancy), hydrodynamic force (fluid inertia and viscous force), propeller thrust and rudder force, and time-varying interference forces (such as wave force and ocean current).

According to the Newton-Euler equation of motion in the fluid, the 6-DOF dynamics equation of AUV with mass m was established in the body-fixed frame:

$$\boldsymbol{M}\dot{\boldsymbol{v}}+\boldsymbol{C}(\boldsymbol{v})\boldsymbol{v}+\boldsymbol{D}(\boldsymbol{v})\boldsymbol{v}+\boldsymbol{G}(\boldsymbol{\eta})=\boldsymbol{\tau}+\boldsymbol{\omega} \tag{10}$$

Where $\boldsymbol{v}$ represents the velocity of AUV in the body-fixed frame; $\boldsymbol{M}\in\boldsymbol{R}^{6\times6}$ is the inertia matrix of AUV system; $\boldsymbol{C}(\boldsymbol{v})\in\boldsymbol{R}^{6\times6}$ is Coriolis centripetal force matrix; $\boldsymbol{D}(\boldsymbol{v})\in\boldsymbol{R}^{6\times6}$ is fluid hydrodynamic damping matrix; $\boldsymbol{G}(\boldsymbol{\eta})\in\boldsymbol{R}^{6\times1}$ is the restoring force (torque) matrix formed by the combined action of gravity and buoyancy; $\boldsymbol{\tau}\in\boldsymbol{R}^{6\times1}$ is the control input generated by the actuator (rudder and propeller); $\boldsymbol{\omega}\in\boldsymbol{R}^{6\times1}$ is the disturbing force brought by external environment such as waves and currents.

3.2.2.1. Kinetic parameter

(1) Inertia matrix

When rigid AUV moves in the fluid medium, it will drive a part of the surface fluid to move at the same time. The mass of this part of the fluid medium can be regarded as generalized mass, and its motion can be regarded as rigid-body motion with the same velocity as AUV. This part of the fluid mass is called additional mass. Therefore, the inertia matrix $\boldsymbol{M}$ of AUV in motion includes the mass of the object itself and the inertia matrix $\boldsymbol{M}_{RB}$ and the additional mass matrix $\boldsymbol{M}_{A}$:

$$\boldsymbol{M}=\boldsymbol{M}_{RB}+\boldsymbol{M}_{A} \tag{11}$$

where $\boldsymbol{M}_{RB}$ is described as

$$\boldsymbol{M}_{RB}=\begin{bmatrix} m & 0 & 0 & 0 & mz_g & -my_g \\ 0 & m & 0 & -mz_g & 0 & mx_g \\ 0 & 0 & m & my_g & -mx_g & 0 \\ 0 & -mz_g & my_g & I_x & -I_{xy} & -I_{xz} \\ mz_g & 0 & -mx_g & -I_{yx} & I_y & -I_{yz} \\ -my_g & mx_g & 0 & -I_{zx} & -I_{zy} & -I_z \end{bmatrix} \tag{12}$$

where m represents the mass of AUV; I represents the moment of inertia of AUV, (x_g, y_g, z_g) represents the position coordinates of AUV in the earth-fixed frame, and $\boldsymbol{M}_{RB}$ satisfies

$$\boldsymbol{M}_{RB} = \boldsymbol{M}_{RB}^{T} > 0, \ \dot{\boldsymbol{M}}_{RB} = 0 \tag{13}$$

$\boldsymbol{M}_A$ is described as:

$$\boldsymbol{M}_A = -\begin{bmatrix} X_{\dot{u}} & X_{\dot{v}} & X_{\dot{w}} & X_{\dot{p}} & X_{\dot{q}} & X_{\dot{r}} \\ Y_{\dot{u}} & Y_{\dot{v}} & Y_{\dot{w}} & Y_{\dot{p}} & Y_{\dot{q}} & Y_{\dot{r}} \\ Z_{\dot{u}} & Z_{\dot{v}} & Z_{\dot{w}} & Z_{\dot{p}} & Z_{\dot{q}} & Z_{\dot{r}} \\ K_{\dot{u}} & K_{\dot{v}} & K_{\dot{w}} & K_{\dot{p}} & K_{\dot{q}} & K_{\dot{r}} \\ M_{\dot{u}} & M_{\dot{v}} & M_{\dot{w}} & M_{\dot{p}} & M_{\dot{q}} & M_{\dot{r}} \\ N_{\dot{u}} & N_{\dot{v}} & N_{\dot{w}} & N_{\dot{p}} & N_{\dot{q}} & N_{\dot{r}} \end{bmatrix} \tag{14}$$

$\boldsymbol{M}_A$ adopts the standard symbol of the Society of Naval Architecture and Marine Engineering (SNAME). For example, the additional mass force along the axis Oz generated by the acceleration $\dot{u}$ of AUV along the axis Ox is

$$Z_u = Z_{\dot{u}}\dot{u} = \frac{\partial Z_u}{\partial \dot{u}}\dot{u} \tag{15}$$

If the AUV is operating entirely underwater, $\boldsymbol{M}_A$ is strictly positive, that is $\boldsymbol{M}_A > 0$.

If AUV is symmetric about oxy, oxz and oyz planes, the inertia matrix $\boldsymbol{M}$ can be written as

$$\boldsymbol{M} = \mathrm{diag}\{m_{11} \ m_{22} \ m_{33} \ m_{44} \ m_{55} \ m_{66}\} \tag{16}$$

(2) Coriolis centripetal force matrix

Coriolis centripetal force matrix $\boldsymbol{C}(\boldsymbol{v})$ consists of rigid centripetal force matrix $\boldsymbol{C}_{RB}(\boldsymbol{v})$ and similar Coriolis moment $\boldsymbol{C}_A(\boldsymbol{v})$ caused by additional mass matrix $\boldsymbol{M}_A$, which is expressed as

$$\boldsymbol{C}(\boldsymbol{v}) = \boldsymbol{C}_{RB}(\boldsymbol{v}) + \boldsymbol{C}_A(\boldsymbol{v}) \tag{17}$$

where $\boldsymbol{C}_{RB}(\boldsymbol{v})$ is described as

$$\boldsymbol{C}_{RB}(\boldsymbol{v})=\begin{bmatrix} 0 & 0 & 0 \\ 0 & 0 & 0 \\ 0 & 0 & 0 \\ -m(y_G q+z_G r) & m(y_G p+w) & m(z_G p-v) \\ m(z_G p-v) & -m(z_G r+x_G p) & m(z_G q+u) \\ m(x_G r+v) & m(y_G r-u) & -m(x_G p+y_G q) \end{bmatrix}$$
$$\begin{bmatrix} m(y_G q+z_G r) & -m(x_G q-w) & -m(x_G r+v) \\ -m(y_G p+w) & m(z_G r+x_G p) & -m(y_G r-u) \\ -m(z_G p-v) & -m(z_G q+u) & m(x_G p+y_G q) \\ 0 & -I_{yz}q-I_{xz}p+I_z r & I_{yz}r+I_{xy}p+I_y q \\ I_{yz}q+I_{xz}p-I_z r & 0 & -I_{xz}r-I_{xy}q+I_x p \\ -I_{yz}r-I_{xy}p+I_y q & I_{xz}r+I_{xy}q-I_x p & 0 \end{bmatrix} \tag{18}$$

It satisfies the condition

$$\boldsymbol{C}_{RB}(\boldsymbol{v})=-\boldsymbol{C}_{RB}^{T}(\boldsymbol{v}) \quad \forall \boldsymbol{v}\in \boldsymbol{R}^{6\times 1} \tag{19}$$

$\boldsymbol{C}_A(\boldsymbol{v})$ can be expressed as

$$\boldsymbol{C}_A(\boldsymbol{v})=-\boldsymbol{C}_A(\boldsymbol{v})^T=\begin{bmatrix} 0 & 0 & 0 & 0 & -a_3 & a_2 \\ 0 & 0 & 0 & a_3 & 0 & -a_1 \\ 0 & 0 & 0 & -a_2 & a_1 & 0 \\ 0 & -a_3 & a_2 & 0 & -b_3 & b_2 \\ a_3 & 0 & -a_1 & b_3 & 0 & -b_1 \\ -a_2 & a_1 & 0 & -b_2 & b_1 & 0 \end{bmatrix} \tag{20}$$

Where

$$\begin{aligned} a_1 &= X_{\dot{u}}u+X_{\dot{v}}v+X_{\dot{w}}w+X_{\dot{p}}p+X_{\dot{q}}q+X_{\dot{r}}r \\ a_2 &= X_{\dot{v}}u+Y_{\dot{v}}v+Y_{\dot{w}}w+Y_{\dot{p}}p+Y_{\dot{q}}q+Y_{\dot{r}}r \\ a_3 &= X_{\dot{w}}u+Y_{\dot{w}}v+Z_{\dot{w}}w+Z_{\dot{p}}p+Z_{\dot{q}}q+Z_{\dot{r}}r \\ b_1 &= X_{\dot{p}}u+Y_{\dot{p}}v+Z_{\dot{p}}w+K_{\dot{p}}p+K_{\dot{q}}q+K_{\dot{r}}r \\ b_2 &= X_{\dot{q}}u+Y_{\dot{q}}v+Z_{\dot{q}}w+K_{\dot{q}}p+M_{\dot{q}}q+M_{\dot{r}}r \\ b_3 &= X_{\dot{r}}u+Y_{\dot{r}}v+Z_{\dot{r}}w+K_{\dot{r}}p+M_{\dot{r}}q+N_{\dot{r}}r \end{aligned} \tag{21}$$

(3) Damping matrix

Real fluids are always viscous. When AUV moves in the fluid, it will be affected by the viscous resistance of the surrounding viscous fluid, which hinders the relative motion between AUV and the fluid.

The main sources of viscous resistance are linear friction of laminar boundary layer, secondary friction of turbulent boundary layer and secondary resistance caused by eddy current. The viscous resistance is a function of relative velocity between AUV and fluid.

In low-velocity navigation of AUV, it is generally assumed that the damping force beyond the second order can be ignored. Then the viscous damping $\boldsymbol{D}(\boldsymbol{v})$ can be written as a matrix composed of linear viscous damping term $\boldsymbol{D}_l$ and nonlinear viscous damping term $\boldsymbol{D}_n(\boldsymbol{v})$:

$$\boldsymbol{D}(\boldsymbol{v}) = \boldsymbol{D}_l + \boldsymbol{D}_n(v) \tag{22}$$

It can be expressed specifically as

$$\boldsymbol{D}(\boldsymbol{v}) = \begin{bmatrix} X_u + X_{u|u|}|u| & 0 & 0 & 0 & 0 & 0 \\ 0 & Y_v + Y_{v|v|}|v| & 0 & 0 & 0 & 0 \\ 0 & 0 & Z_w + Z_{w|w|}|w| & 0 & 0 & 0 \\ 0 & 0 & 0 & K_p + K_{p|p|}|p| & 0 & 0 \\ 0 & 0 & 0 & 0 & M_q + M_{q|q|}|q| & 0 \\ 0 & 0 & 0 & 0 & 0 & N_r + N_{r|r|}|r| \end{bmatrix} \tag{23}$$

Where the linear damping term $\boldsymbol{D}_l$ and nonlinear damping term $\boldsymbol{D}_n(\boldsymbol{v})$ are:

$$\boldsymbol{D}_l = \mathrm{diag}\{X_u \;\; Y_v \;\; Z_w \;\; K_p \;\; M_q \;\; N_r\} \tag{24}$$

$$\boldsymbol{D}_n(\boldsymbol{v}) = \mathrm{diag}\{X_{u|u|}|u| \;\; Y_{v|v|}|v| \;\; Z_{w|w|}|w| \;\; K_{p|p|}|p| \;\; M_{q|q|}|q| \;\; N_{r|r|}|r|\} \tag{25}$$

respectively.

3.2.2.2. Restoring force (moment)

Restoring force is a fluid dynamics term that refers to the static force of the AUV's underwater motion -- gravity W and buoyancy B, acting on the AUV's barycenter $r_G = (x_G, y_G, z_G)$ and floating center $r_B = (x_B, y_B, z_B)$, respectively.

According to the Institute of SNAME standards, gravity is defined as $W = mg$ and buoyancy is defined as $B = \rho g \nabla$. When AUV is completely immersed in the fluid, the gravity vector f_G and buoyancy vector f_B are expressed in the body-fixed frame as:

$$f_G(\boldsymbol{\eta}_2)=\boldsymbol{J}_1^{-1}(\boldsymbol{\eta}_2)\begin{bmatrix}0\\0\\W\end{bmatrix},\ f_B(\boldsymbol{\eta}_2)=-\boldsymbol{J}_1^{-1}(\boldsymbol{\eta}_2)\begin{bmatrix}0\\0\\B\end{bmatrix} \tag{26}$$

In the body-fixed frame, the positive direction of axis Oz is downward, then the restoring force and torque vector $\boldsymbol{g}(\boldsymbol{\eta})$ suffered by AUV are

$$\boldsymbol{g}(\boldsymbol{\eta})=-\begin{bmatrix}f_G(\boldsymbol{\eta})+f_B(\boldsymbol{\eta})\\r_G\times f_G(\boldsymbol{\eta})+r_B\times f_B(\boldsymbol{\eta})\end{bmatrix} \tag{27}$$

Substituting (26) into (27), the expansion form of restoring force and torque $\boldsymbol{g}(\boldsymbol{\eta})$ is obtained as follows:

$$\boldsymbol{g}(\boldsymbol{\eta})=\begin{bmatrix}(W-B)\sin\theta\\-(W-B)\sin\varphi\cos\theta\\-(W-B)\cos\varphi\cos\theta\\-(y_GW-y_BB)\cos\theta\cos\varphi+(z_GW-z_BB)\cos\theta\sin\varphi\\(z_GW-z_BB)\sin\theta+(x_GW-x_BB)\cos\theta\cos\varphi\\-(x_GW-x_BB)\cos\theta\sin\varphi-(y_GW-y_BB)\sin\theta\end{bmatrix} \tag{28}$$

When the AUV under study satisfies neutral equilibrium, namely $W=B$, the distance variable between the center of gravity and the center of buoyancy is defined as

$$\overline{BG}=\begin{bmatrix}\overline{BG_x}\\\overline{BG_y}\\\overline{BG_z}\end{bmatrix}=\begin{bmatrix}x_G-x_B\\y_G-y_B\\z_G-z_B\end{bmatrix}^T \tag{29}$$

At this point, $\boldsymbol{g}(\boldsymbol{\eta})$ can be rewritten as:

$$\boldsymbol{g}(\boldsymbol{\eta})=\begin{bmatrix}0\\0\\0\\-\overline{BG_y}W\cos\theta\cos\varphi+\overline{BG_Z}W\cos\theta\sin\varphi\\\overline{BG_z}W\sin\theta+\overline{BG_x}W\cos\theta\cos\varphi\\-\overline{BG_x}W\cos\theta\sin\varphi-\overline{BG_y}W\sin\theta\end{bmatrix} \tag{30}$$

3.2.2.3. Main force

AUV is usually driven by a thruster-rudder to achieve motion control.

Fully actuated AUV has more lateral thrusters than underactuated AUV. The forward direction movement is controlled by the tail propeller, which adjusts the thrust force by adjusting the propeller speed, so as to realize the forward direction speed control.

The motion control of the vertical direction and horizontal direction is realized by adjusting the rudder angle, which includes the horizontal rudder and vertical rudder. The horizontal rudder controls the pitch angle, and the vertical rudder controls the yaw angle. The rudders realize the control of AUV sailing depth and direction collaborating with the tail propeller.

(1)Propulsive force

Normally, an underactuated AUV has two propellers at tail, and the longitudinal thrust generated by the left and right propellers is:

$$X_{prop} = X_{TL} + X_{TR} \tag{31}$$

Where X_{TL} and X_{TR} are the thrust generated by the left and right thrusters of AUV respectively.

According to hydrodynamic test, the relationship between thruster thrust and steering gear speed can be derived:

$$X_P = C_n n|n| \tag{32}$$

Where X_P represents the thrust of a single propeller, C_P represents the relationship coefficient between thrust and speed, and n represents the actual rotate speed of the propeller.

The rotational characteristics of propeller can be described by first-order inertia model:

$$n = K_M (n_r - n)/T_M \tag{33}$$

Where K_M is the control gain parameter, T_M is the time constant, and n_r is the target command rotate speed.

(2)Deflection moment

The pitch moment generated by the horizontal rudder and the yaw moment generated by the vertical rudder are:

$$M = \frac{1}{2}\rho L^4 M_{|q|\delta_s}^{\cdot} u|q|\delta_s + \frac{1}{2}\rho L^3 M_{\delta_s}^{\cdot} u^2 \delta_s \tag{34}$$

$$N = \frac{1}{2}\rho L^4 N_{|r|\delta_r}^{\cdot} u|r|\delta_r + \frac{1}{2}\rho L^3 N_{\delta_r}^{\cdot} u^2 \delta_r \tag{35}$$

where, δ_s and δ_s are real-time rudder angles of horizontal and vertical rudder at work, and $M_{(\cdot)}^{\cdot}$ and $N_{(\cdot)}^{\cdot}$ are dimensionless hydrodynamic coefficients of horizontal and vertical directions respectively.

3.2.3. Horizontal mathematical model of underactuated AUV

In this thesis, the motion control of AUV (single and formation) in horizontal plane is studied. In order to facilitate the design of the controller, this thesis simplifies the 6-DOF space motion model, which is a complex multi-variable nonlinear system, and obtains a plane motion model which only considers the surge, sway and yaw.

The horizontal motion of the underactuated AUV can be described by coordinate vectors $\boldsymbol{\eta} = [x, y, z]^T$ and velocity vectors $\boldsymbol{v} = [u, v, r]^T$.

Combined with literature (Do, Jiang & Pan, 2002) the horizontal mathematical model of AUV is expressed as follows:

$$\begin{aligned} \dot{\boldsymbol{\eta}} &= \boldsymbol{J}(\psi)\boldsymbol{v} \\ \boldsymbol{M}\dot{\boldsymbol{v}} &= -\boldsymbol{C}(\boldsymbol{v})\boldsymbol{v} - \boldsymbol{D}(\boldsymbol{v})\boldsymbol{v} + \boldsymbol{\tau} \end{aligned} \tag{36}$$

Some assumptions about AUV under ideal conditions are as follows:

(1) AUV mass distribution is uniform;

(2) AUV's center of gravity coincide with the center of buoyancy, and the magnitude of gravity and buoyancy is equal;

(3) Both vertical parameters z, w, θ, q and roll motion parameters φ, p are assumed to be 0;

(4) AUV is symmetric in front and rear, left and right, and up and down, so inertia matrix and hydrodynamic damping matrix are diagonal matrix;

(5) Ignore the time-varying interference of wind, wave and ocean current drift.

Then, the horizontal kinematics equation of underactuated AUV is:

$$\begin{bmatrix} \dot{x} \\ \dot{y} \\ \dot{\psi} \end{bmatrix} = \begin{bmatrix} \cos\psi & -\sin\psi & 0 \\ \sin\psi & \cos\psi & 0 \\ 0 & 0 & 1 \end{bmatrix} \begin{bmatrix} u \\ v \\ r \end{bmatrix} \tag{37}$$

Its expansion formula is:

$$\begin{cases} \dot{x} = u\cos\psi - v\sin\psi \\ \dot{y} = u\sin\psi + v\cos\psi \\ \dot{\psi} = r \end{cases} \tag{38}$$

The horizontal plane dynamics equation of underactuated AUV can be expressed as:

$$\begin{cases} \dot{u} = \dfrac{m_{22}}{m_{11}} vr - \dfrac{d_{11}}{m_{11}} u + \dfrac{\tau_u}{m_{11}} \\ \dot{v} = -\dfrac{m_{11}}{m_{22}} ur - d_{22} v \\ \dot{r} = -\dfrac{m_{22} - m_{11}}{m_{33}} uv - d_{33} r + \dfrac{\tau_r}{m_{11}} \end{cases} \tag{39}$$

Where, $m_{11} = m - X_{\dot{u}}, m_{22} = m - Y_{\dot{v}}, m_{33} = I_z - N_{\dot{r}}$. τ_u and τ_r represent control inputs.

For convenience, equation (39) is written as:

$$\begin{cases} \dot{u} = \dfrac{1}{c} vr - au + \tau_1 \\ \dot{v} = -cur - bv \\ \dot{r} = kuv - dr + \tau_2 \end{cases} \tag{40}$$

The constants are defined as follows:

$$\tau_1 = \frac{1}{m_{11}} \tau_u,\ \tau_2 = \frac{1}{m_{33}} \tau_r$$

$$a = \frac{d_{11}}{m_{11}}, b = \frac{d_{22}}{m_{22}}, c = \frac{m_{11}}{m_{22}},\ d = \frac{d_{33}}{m_{33}},\ \kappa = \frac{m_{11} - m_{22}}{m_{33}}$$

τ_1, τ_2 are the control inputs with saturation limitation.

3.3. Theories related to nonlinear system control

The control system in the actual operation of the process is always affected by environmental interference. If the system cannot effectively maintain stability, the system will have a great hidden danger, so the study of system stability is of great significance.

The Lyapunov stability theory of Russian mathematician Lyapunov can be applied to analyze the stability of linear system and nonlinear system, steady system and time-varying system at the same time. It is also the most commonly used method to study nonlinear control system at present.

Lyapunov stability theory mainly refers to Lyapunov's second method, which is not limited to local motion. It evaluates the stability by observing the change of the function with time, which constructed by the variable to be analyzed of the system. This method does not need to solve the equation of state of the system, but can directly judge the stability, and is applicable to the system of any order.

Definition 2.1 equilibrium point: for nonlinear system $\dot{x} = f(t,x)$, if $x = 0$ is the equilibrium point of the system, then there is $\forall t \geqslant 0$ so that $f(t,0) = 0$.

Definition 2.2 Stability: if there is a positive constant r and a $\mathcal{K}$-class function α, making the solution of the nonlinear system $\dot{x} = f(t,x)$ satisfies the relation:

$$\|x(t)\| \leqslant \alpha(\|x(t_0)\|),\ \forall t \geqslant t_0 \geqslant 0,\ \ \forall \|x(t_0)\| \leqslant r(t_0) \tag{41}$$

Then the equilibrium point of the system $x = 0$ is stable.

Definition 2.3 Asymptotically stable: if there is a positive constant r and a $\mathcal{KL}$-class function β, making the solution of the nonlinear system $\dot{x} = f(t,x)$ satisfies the relation:

$$\|x(t)\| \leqslant \beta(\|x(t_0)\|, t - t_0),\ \forall t \geqslant t_0 \geqslant 0,\ \ \forall \|x(t_0)\| \leqslant r(t_0) \tag{42}$$

The equilibrium point of the system $x = 0$ is local asymptotic stable.

If $r(t_0) \to \infty$, the equilibrium point $x = 0$ is said to be globally asymptotically stable.

Definition 2.4 Exponential stable: if there are positive constants k, λ and $r(t_0)>0$ making the solution of the nonlinear system $\dot{x}=f(t,x)$ satisfies the relation:

$$\|x(t)\|\leqslant k\|x(t_0)\|e^{-\lambda(t-t_0)},\ \forall t\geqslant t_0\geqslant 0,\ \ \forall\|x(t_0)\|\leqslant r(t_0) \tag{43}$$

The equilibrium point of the system $x=0$ is local exponential stable. If $r(t_0)\to\infty$, the equilibrium point $x=0$ is said to be globally exponential stable. Where λ represents the speed of convergence.

If the above positive constant r are independent of t_0, the above properties are uniformly true.

The relevant lemmas in the sense of Lyapunov stability are introduced below.

Lemma 2.1 For a nonlinear system $\dot{x}=f(t,x)$,let $x=0\in D\in R^n$ be the equilibrium point of the system. If there is a continuous and differentiable scalar function $V(t,x)$,the following relations are satisfied for all $\forall t>0$:

$$\alpha_1(\|x\|)\leqslant V(t,x)\leqslant\alpha_2(\|x\|) \tag{44}$$

$$\frac{\partial V}{\partial t}+\frac{\partial V}{\partial x}f(t,x)\leqslant-\alpha_3(\|x\|) \tag{45}$$

where $\alpha_i(i=1,2,3)$ are $\mathcal{K}$ -class function, the equilibrium point $x=0$ is uniformly asymptotically stable. If $D\in R^n$ and $\alpha_1\in\mathcal{K}_\infty$, the equilibrium point $x=0$ is globally uniformly asymptotically stable.

Lemma 2.2 For a nonlinear system $\dot{x}=f(t,x)$, let $x=0\in D\in R^n$ be the equilibrium point of the system. If there is a continuous and differentiable scalar function $V(t,x)$, satisfy the following relations for all $\forall t>0$:

$$k_1\|x(t)\|^a\leqslant V(t,x)\leqslant k_2\|x(t)\|^a \tag{46}$$

$$\frac{\partial V}{\partial t}+\frac{\partial V}{\partial x}f(t,x)\leqslant-k_3\|x(t)\|^a \tag{47}$$

where $k_i(i=1,2,3)>0$, $a>0$, we say the equilibrium point is exponentially stable. If the above assumptions are globally true, we can say the equilibrium point $x=0$ is globally exponentially stable.

However, to reach the conclusion of the lemma, more stringent conditions must be met. For example, when using Lyapunov stability theory to analyze the stability of the system, it is required that the derivative value of the function $\dot{V}(x)$ must be negative definite. However, in practical application, Lyapunov function is usually semi-negative definite, so the above lemma cannot be used to analyze the stability of the control system.

Therefore, Babalat's lemma with looser conditions and Lasalle invariant set principle are more commonly used in the analysis process.

Lemma 2.3 Barbalet's lemma: Let $f:R^+ \to R$ be a uniformly continuous function, if $\lim_{t\to\infty}\int_0^t f(\tau)d\tau$ exists and is finite, then $\lim_{t\to\infty} f(t)=0$.

Lemma 2.4 Corollary of Barbalet's lemma: if a positive definite function $V(t)$ is second differentiable, $\lim_{t\to\infty} V(t)=\delta$ (δ is nonnegative function), and $\ddot{V}(t)$ exists and is bounded, then $\lim_{t\to\infty}\dot{V}(t)=0$.

Lemma 2.5 Lasalle invariant set principle: let Λ be invariant set of nonlinear system $\dot{x}=f(t,x)$, if any solution starting from invariant set Λ can converge to set $E\subset A$, then when $t\to\infty$,any solution starting from the invariant set Λ can asymptotically converge to M (where M is the largest invariant subset of E).

3.4. Common AUV control methods

Many scholars have conducted many studies on the motion control of AUV and proposed corresponding solutions, which can be divided into the following categories:

(1) PID control

A linear control method. The desired value and the actual output form a deviation. The controller is composed of a linear combination of Proportion, Integral and Differential parts of the deviation.

PID controller is simple in structure and easy to implement, and is especially widely used in practical engineering. However, it is difficult to obtain ideal control effect when dealing with nonlinear systems like AUV, so local linearization is usually adopted or combined with other control strategies to improve it (Khodayari & Balochian, 2015).

(2) Backstepping

A recursive design method that divides the higher-order system into several interrelated subsystems, builds the Lyapunov function step by step by step, and designs the virtual control function in the middle to stabilize the subsystems at the previous level.

Backstepping method also has its limitations. In the design process, the derivative of the intermediate virtual controller needs to be calculated step by step. When the formal complexity of virtual control increases or the system order increases, the derivation process will be very complicated (Yang, Jie & Yue, 2002).

(3) Adaptive control

The model of underwater vehicle includes the mathematical structure of the model and the parameters of the model. Because it is difficult to accurately estimate the structural parameters of the model, there are always deviations. At the same time, the change of time brings uncertainty to parameters and may also change the model structure of the AUV (Li & Lee, 2005).

Adaptive control has time-varying parameters and can constantly correct the parameter changes of the controlled signal, so it can adapt to the model errors of the system and deal with the disturbance of the dynamic model.

However, the adaptive control can only control the system with parameters varying in a certain range, and the adaptive law is easily affected by many factors, especially bounded interference.

(4) Sliding-mode control

It is a special kind of nonlinear control, and the nonlinearity is mainly the discontinuity of control. Under this control strategy, the "structure" of the system is not fixed, and the control input will constantly change according to the current state of the system in the dynamic process, forcing the system to constantly approach the pre-designed sliding mode surface, crossing back and forth on the sliding mode surface, and then making the system move to the equilibrium point of the system in accordance with the state track of the predetermined sliding mode.

The advantages of sliding mode variable structure control are fast response speed, adaptive to system perturbation and external disturbance, no need for online identification and simple physical implementation.

However, after the state trajectory reaches the sliding mode surface, it will chatter back and forth on both sides of the sliding mode surface, affecting the control accuracy (Liu & Sun, 2007). The shortcoming of chattering phenomenon needs to be overcome by sliding mode control combined with other control methods.

(5) Fuzzy control

The main idea is to establish a model simulating human control experts, so that they can control the controlled object without considering the mathematical model (Akkizidis & Roberts, 1998).

Fuzzy control has strong anti-interference and robustness to the uncertainty of nonlinear system, and its physical implementation is relatively simple, but it does not have adaptive ability, so it needs to be combined with adaptive control or other control methods.

(6) Neural network control

An information processing system that mimics the structure and function of the biological brain.

Multi-layer neural network system consists of neurons with simple structure and function. It can approach arbitrary complex nonlinear system and carry out online autonomous learning, memory, association and identification. Using weight to adapt and adjust the system dynamic characteristics, neural network control can be applied to complex system modeling, state estimation, overcoming the strong interference and uncertainty and online optimization (Hunt, Sbarbaro, Zbikowski & Gawthrop, 1992).

However, due to the short development time, a lot of practical experience is still needed in terms of node number, network type and hidden layer setting.

3.5. Common multi-AUV formation control method

At present, the common multi-AUV formation control methods mainly include the following:

(1)Formation control based on Leader-follower

This method means that in a multi-AUV system, one or several individual AUVs are selected as the leader of a formation, and the other AUVs act as followers, so as to follow the main body by communicating with their neighbors.

The key point of this strategy is to obtain the information of leader's position and attitude and let followers track them, so that the problem of formation control can be transformed into a problem of target-tracking. However, the disadvantage of this method is also obvious, that is, it relies heavily on the leader -- once the leader fails, the whole formation fails.

(2)Formation control based on Artificial Potential Field

The basic idea of this method is to set up a virtual potential field, which will produce different repulsive and gravitation forces to individuals at different positions in the field, so as to adjust the relative position of each AUV in the team and the distance between target points or obstacles, so that the AUV formation can reach the desired formation state.

The advantage of the artificial potential field method is that, as long as the potential field function is determined, the rest of the calculation is relatively simple, which can realize the

real-time control of the formation and complete the complex tasks such as obstacle avoidance and formation shape adjustment of the AUV formation under the complex sea area. The disadvantage is that the potential field function is difficult to design.

(3)Formation control based on virtual structure

This method generates a virtual rigid body structure through some algebraic operations on the states of all AUV individuals, and then the whole AUV formation is regarded as a rigid body. The desired position and trajectory of each individual are calculated by the position of the reference point and the desired formation configuration.

The disadvantage of this method is that it lacks flexibility and adaptability, and the state data operation needs to be processed centrally, so it is only suitable for small formation system.

(4)Formation control based on behavior

This method belonging to the idea of distributed method. the formation control task is decomposed into a series of basic behaviors, and an appropriate control law is predefined for each AUV individual, so that it can correspond to all possible states of AUV individual, and the control of the overall movement of AUV formation is realized by synthesizing basic behaviors.

Its disadvantage is that the group behavior is difficult to define, the quantitative mathematical analysis in the next step is difficult to achieve.

(5)Formation control based on Graph

This method makes one-to-one correspondence between nodes on the graph and the physical position of AUV. Generally, directed line between two nodes is used to correspond to the transfer relation of information. Many directed lines form a control diagram, and the individual position and constraint relation in AUV formation are described by it.

In this method, graph theory is mainly used to reflect the structure of formation system, analyze the constraints and communication relations between AUVs, and directly reflect the change of constraints and communication between individual AUVs in formation architecture or formation transformation.

The advantage of this method is that the graph theory is mature, and it can describe the formation and communication of any AUV formation, but the disadvantage is that it is difficult to implement.

3.6. Multi-AUV formation strategy

A multi-AUV formation can usually be defined in two ways: one is defined according to the position of the AUV in a specific coordinate system (such as the relative position of the follower in the leader's body-fixed frame), and the other is defined according to the geometry formed by the AUV inside the formation.

Complex formations of multiple AUVs can be decomposed into three basic formations, which are:

(1) Single leader-single follower formation;

(2) Double leaders-single follower formation;

(3) Single leader-double followers' formation.

In single-leader-single-follower mode, the Leader sends its position information to the follower through the communication device carried by itself. After receiving the status information, the follower moves to a specific position in the leader's body-fixed frame according to the preset control rules. It belongs to the formation defined by the first method.

The essences of the two types of structures, double leaders-single follower and single leader-double follower are the same, that is to control the movement of individuals in the formation according to the distance information, so as to form a specific geometric formation, which belongs to the formation defined by the second method.

In this thesis, the AUV formation is composed of three AUVs. The formation structure is controlled by the first definition -- the position of the AUV in a specific coordinate system. The formation is divided into two basic formation structures of single leader-single follower. The follower has been set at the desired position on the leader's body-fixed frame in advance, and formation control can be carried out after calculation combined with the received leader state

Chapter 4. Results - Simultaneous tracking and stabilization control of single underactuated AUV

Most studies on AUV motion control include only one task: trajectory tracking or point stabilization, and there are relatively few designs that can accomplish both tasks without switching controllers.

In this thesis, a saturation dynamics controller is designed for both trajectory tracking and point stabilization, which avoids the problem of too many and too complex parameters brought by the traditional backstepping controller.

Based on the existing controller, the event triggering mechanism and event triggering controller are designed, so as to reduce the execution times of power actuator and improve the economy of AUV control on the premise of ensuring the reliability of the system.

4.1. Problem description

By designing saturation control input $\tau_1,\ \tau_2$, the underactuated AUV realizes simultaneous tracking and stabilization control. In other words, the underactuated AUV expressed by Equations (3.38) and (3.39) is driven to make the trajectory $\boldsymbol{\eta} = [x, y, \psi]^T$ track an arbitrary smooth desired trajectory $\boldsymbol{\eta}_d = [x_d, y_d, \psi_d]^{\boldsymbol{T}}$ and ensure that the tracking error $\boldsymbol{\eta}_d - \boldsymbol{\eta}$ converges to a bounded region near zero point. The desired trajectory can be either time-varying trajectory (tracking) or fixed point (point stabilization).

4.2. Controller design and stability proof

Suppose that the desired trajectory is generated by the kinematic equation of a virtual underactuated AUV, which is similar to the original AUV model:

$$\begin{cases} \dot{x}_d = u_d \cos\psi_d - v_d \sin\psi_d \\ \dot{y}_d = u_d \sin\psi_d + v_d \cos\psi_d \\ \dot{\psi}_d = r_d \\ \dot{v}_d = -cu_d r_d - bv_d \end{cases} \tag{48}$$

In order to facilitate the design of the controller, the error variables are obtained by coordinate transformation:

$$\begin{bmatrix} x_e \\ y_e \\ \psi_e \end{bmatrix} = \begin{bmatrix} \cos\psi & \sin\psi & 0 \\ -\sin\psi & \cos\psi & 0 \\ 0 & 0 & 1 \end{bmatrix} \begin{bmatrix} x - x_d \\ y - y_d \\ \psi - \psi_d \end{bmatrix} \tag{49}$$

Take the derivative of (49) with respect to time to obtain the tracking error equation:

$$\begin{bmatrix} \dot{x}_e \\ \dot{y}_e \end{bmatrix} = r \begin{bmatrix} 0 & 1 \\ -1 & 0 \end{bmatrix} \begin{bmatrix} x_e \\ y_e \end{bmatrix} + \begin{bmatrix} u \\ v \end{bmatrix} - \begin{bmatrix} \cos(\psi - \psi_d) & \sin(\psi - \psi_d) \\ -\sin(\psi - \psi_d) & \cos(\psi - \psi_d) \end{bmatrix} \begin{bmatrix} u_d \\ v_d \end{bmatrix} \tag{50}$$

$$\dot{\psi}_e = \dot{\psi} - \dot{\psi}_d$$

Define AUV velocity error as:

$$\begin{aligned} u_e &= u - u_d \\ v_e &= v - v_d \\ r_e &= r - r_d \end{aligned} \tag{51}$$

The derivative of velocity error with respect to time can be obtained:

$$\begin{aligned} \dot{u}_e &= \frac{r}{c} v_e - a u_e + \tau_1 - \dot{u}_d + \frac{r}{c} v_d - a u_d \\ \dot{v}_e &= -rcu_e - bv_e - cu_d (r - r_d) \\ \dot{r}_e &= \dot{r} - \dot{r}_d = \kappa uv - dr + \tau_2 - r_d \end{aligned} \tag{52}$$

For the convenience of controller design, matrix transformation can be introduced for coordinate and velocity errors:

$$\begin{bmatrix} z_1 \\ z_2 \end{bmatrix} = \begin{bmatrix} x_e \\ y_e \end{bmatrix} + \begin{bmatrix} \rho & 0 \\ 0 & \rho/c \end{bmatrix} \begin{bmatrix} u_e \\ v_e \end{bmatrix} \tag{53}$$

Derivate it and we can obtain:

$$\begin{bmatrix} \dot{z}_1 \\ \dot{z}_2 \end{bmatrix} = r \begin{bmatrix} 0 & 1 \\ -1 & 0 \end{bmatrix} \begin{bmatrix} z_1 \\ z_2 \end{bmatrix} + \begin{bmatrix} 1-a\rho & 0 \\ 0 & 1-b\rho/c \end{bmatrix} \begin{bmatrix} u_e \\ v_e \end{bmatrix} + \begin{bmatrix} \rho(\tau_1 - \dot{u}_d + rv_d/c - au_d) \\ -\rho u_d (r - r_d) \end{bmatrix} + \begin{bmatrix} F_1(\psi - \psi_d) \\ F_2(\psi - \psi_d) \end{bmatrix} \tag{54}$$

Where $F_1(\psi - \psi_d)$ and $F_2(\psi - \psi_d)$ are the function of $\psi - \psi_d$

$$\begin{cases} F_1(\psi - \psi_d) = -\cos(\psi - \psi_d) u_d - \sin(\psi - \psi_d) v_d + u_d \\ F_2(\psi - \psi_d) = \sin(\psi - \psi_d) u_d - \cos(\psi - \psi_d) v_d + v_d \end{cases} \tag{55}$$

At this point, the control objective of this paper can be transformed into follows: by designing suitable τ_1 and τ_2, the tracking error (z_1, z_2) and (ψ_e, r_e) converges to a bounded neighborhood near the zero point.

As can be seen from the above, AUV system has a strict feedback form, so Lyapunov's second method can be used for controller design.

For the convenience of model controller design, the tracking error system can be divided into two cascaded subsystems: yaw subsystem $\Sigma_1: [\psi_e, r_e]^T$ and propulsion subsystem $\Sigma_2: [z_1, z_2]^T = [x_e + \rho u_e, y_e + \rho u_e/c]^T$, and the corresponding control input τ_2 and τ_1 are designed respectively.

4.2.1. Yaw system control

The motion model of the yaw system can be expressed as:

$$\begin{cases} \dot{\psi}_e = r_e \\ \dot{r}_e = \dot{r} - \dot{r}_d = \kappa uv - dr + \tau_2 - r_d \end{cases} \tag{56}$$

In the process of AUV performing stabilization tasks, when the propulsion subsystem has not realized stabilization, it is necessary to ensure that the angular velocity is continuously excited, so as to avoid the failure of τ_2 when the Angle reaches the desired value at some moment, so that AUV cannot continue to be control to reach the desired position only by τ_1.

Therefore, the variable $\delta(t)$ is introduced as the additional control term, and t is defined by the following second-order differential equation:

$$\ddot{\delta} + 2C_\delta \dot{\delta} + C_\delta^2 \delta = k_\delta h(t) \tanh\{[(g(t) + u_d) z_2]\} \tag{57}$$

Where, C_δ and C_δ are appropriate positive constants; $h(t)$ and $g(t)$ respectively satisfy:

$$\dot{h} = -k_h r_d^2 h, \quad h(0) = 1 \tag{58}$$

$$\ddot{g} = -k_g u_d^2 \dot{g} - g, \; g(0) = 1 \tag{59}$$

Likewise, k_h and k_g are properly positive constants.

According to the definition, when the stabilization task $u_d = r_d = 0$ is performed, δ will provide a small amount of fluctuation before the error variable $z_2 = 0$, so that the AUV can maintain excited continuously in the stabilization process and avoid yaw controller failure.

Add a small variable $\delta(t)$ to the error:

$$\bar{\psi}_e = \psi - \psi_d + \delta(t) \tag{60}$$

A new control model expression can be obtained by taking derivatives of them successively:

$$\begin{cases} \dot{\bar{\psi}}_e = \bar{r}_e = r - r_d + \dot{\delta} \\ \dot{\bar{r}}_e = \dot{r} - \dot{r}_d + \ddot{\delta} = \kappa uv - dr + \tau_2 - \dot{r}_d + \ddot{\delta} \end{cases} \tag{61}$$

Based on the above model, the design control input is as follows:

$$\tau_2 = -\kappa uv + \dot{r}_d - \ddot{\delta} + d\left(r_d - \dot{\delta}\right) - k_r \tanh\left(\bar{r}_e + \bar{\psi}_e\right) \tag{62}$$

Where k_r is a positive constant, τ_2 is limited by saturation and has an upper bound $\tau_{2,\max}$, which will be proved below.

Next step is the stability analysis.

Substitute equation (62) into equation (61) and it is can be obtained that

$$\begin{cases} \dot{\bar{\psi}} = \bar{r}_e \\ \dot{\bar{r}}_e = -dr_e - \tanh(r_e + \psi_e) \end{cases} \tag{63}$$

Set a new error variable:

$$z_3 = \bar{\psi}_e + \bar{r}_e \tag{64}$$

Construct a new Lyapunov function:

$$V_3 = \frac{1}{2}\bar{r}_e + \ln[\cosh(z_3)] > 0 \tag{65}$$

The derivative can be obtained:

$$\begin{aligned} \dot{V}_3 &= -d\bar{r}_e^2 - d\bar{r}_e \tanh(z_3) - \tanh^2(z_3) \\ &= -\frac{1}{2}d\bar{r}_e^2 - \frac{1}{2}d(\bar{r}_e + \tanh(z_3))^2 - \left(\sqrt{1-d}\tanh(z_3)\right)^2 \leq 0 \end{aligned} \tag{66}$$

We know from the above equation that $V_3 > 0$, $\dot{V}_3 \leq 0$. According to Lyapunov's theorem and Barbalat's lemma, $\bar{r}_e$ and z_3 converge asymptotically to a bounded region near zero. According to Equation (64), $\bar{\psi}_e = z_3 - \bar{r}_e$, it can be seen that ψ_e will converge gradually to the bounded region near zero.

4.2.2. Propulsion system control

Consider the control model of the propulsion subsystem Σ_2 :

$$\begin{bmatrix} z_1 \\ z_2 \end{bmatrix} = \begin{bmatrix} x_e \\ y_e \end{bmatrix} + \begin{bmatrix} \rho & 0 \\ 0 & \rho/c \end{bmatrix} \begin{bmatrix} u_e \\ v_e \end{bmatrix} \tag{67}$$

$$\begin{bmatrix} \dot{z}_1 \\ \dot{z}_2 \end{bmatrix} = r\begin{bmatrix} 0 & 1 \\ -1 & 0 \end{bmatrix}\begin{bmatrix} z_1 \\ z_2 \end{bmatrix} + \begin{bmatrix} 1-a\rho & 0 \\ 0 & 1-b\rho/c \end{bmatrix}\begin{bmatrix} u_e \\ v_e \end{bmatrix} + \begin{bmatrix} \rho(\tau_1 - \dot{u}_d + rv_d/c - au_d) \\ -\rho u_d(r - r_d) \end{bmatrix} + \begin{bmatrix} F_1(\psi - \psi_d) \\ F_2(\psi - \psi_d) \end{bmatrix} \tag{68}$$

where

$$\begin{aligned} F_1(\psi - \psi_d) &= -\cos(\psi - \psi_d)u_d - \sin(\psi - \psi_d)v_d + u_d \\ F(\psi - \psi_d) &= \sin(\psi - \psi_d)u_d - \cos(\psi - \psi_d)v_d + v_d \end{aligned} \tag{69}$$

Substitute equation (63) into it, equation (68) can also be written in the following form:

$$\begin{bmatrix}\dot{z}_1\\ \dot{z}_2\end{bmatrix}=r\begin{bmatrix}0 & 1\\ -1 & 0\end{bmatrix}\begin{bmatrix}z_2\\ z_2\end{bmatrix}+\begin{bmatrix}1-a\rho & 0\\ 0 & 1-b\rho/c\end{bmatrix}\begin{bmatrix}u_e\\ v_e\end{bmatrix}+\begin{bmatrix}\rho(\tau_1-\dot{u}_d+rv_d/c-au_d)\\ -\rho u_d\left(\bar{r}_e-\dot{\delta}\right)\end{bmatrix}+\begin{bmatrix}f_1(\delta)\\ f_2(\delta)\end{bmatrix}+\begin{bmatrix}F_1\left[\bar{\psi}_e\right]\\ F_2\left[\bar{\psi}_e\right]\end{bmatrix} \quad (70)$$

Where $f_1(\delta)$ and $f_2(\delta)$ are expressed in the following forms respectively:

$$\begin{aligned}f_1(\delta)&=u_d(1-\cos\delta)+v_d\sin\delta\\ f_2(\delta)&=-u_d\sin\delta+v_d(1-\cos\delta)\end{aligned} \quad (71)$$

Let $1-b\rho/c=0$ be true, then $\rho=c/b$.

According to the above model, the control input τ_u is designed as follows:

$$\tau_1=\dot{u}_d+au_d+\frac{-r_d+\dot{\delta}}{c}v_d-\frac{f_1(\delta)+(1-a\rho)u_e}{\rho}-k_u\tanh(z_1) \quad (72)$$

Where k_u is a positive constant, τ_1 is limited by saturation requirement and has an upper bound $\tau_{1,\max}$, which will be proved below.

Let's do the stability analysis.

For the propulsion system (67) (70), the following Lyapunov function is selected:

$$V_4=\frac{1}{2}z_1^2+\frac{1}{2}z_2^2 \quad (73)$$

Substitute it into equation (70) (71) (72), then we get

$$\dot{V}_4=z_1\frac{\rho\dot{\delta}v_d}{c}-z_1\rho k_u\tanh(z_1)-z_2\rho u_d\left(\bar{r}_e-\dot{\delta}\right)+z_2f_2(\delta)+z_1F_1\left(\bar{\psi}_e\right)+z_2F_2\left(\bar{\psi}_e\right) \quad (74)$$

It has been proved above that $\bar{r}_e$, $\bar{\psi}_e$ asymptotically converge to 0, so equation (74) can also be written as:

$$\dot{V}_4=z_1\frac{\rho\dot{\delta}v_d}{c}-z_1\rho k_u\tanh(z_1)+z_2\rho u_d\dot{\delta}+z_2f_2(\delta) \quad (75)$$

The stability analysis of propulsion subsystem will be discussed in the following three cases:

(1)Case 1: Point stabilization, $r_d = 0,\ u_d = 0,\ v_d = 0$

According to the expression (74) (58), $f_2(\delta) = 0,\ h = 1$, then equation (57) can be written as:

$$\ddot{\delta} + 2C_\delta \dot{\delta} + C_\delta^2 = k\tanh(gz_2) \tag{76}$$

The expression shows that $\ddot{\delta} \to 0,\ \dot{\delta} \to 0$ so (75) can be further simplified as:

$$\dot{V}_4 = -\rho k_u z_1 \tanh(z_1) \leqslant 0 \tag{77}$$

(2)Case 2: linear tracking $r_d = 0,\ u_d \neq 0,\ v_d = 0$

According to the expression (71) (58) (69), $f_2(\delta) = -u_d \sin\delta,\ h = 1,\ g \to 0$, then (57) can be written as:

$$\ddot{\delta} + 2C_\delta \dot{\delta} + C_\delta^2 \delta = k\tanh(u_d z_2) \tag{78}$$

According to the expression, $\ddot{\delta} \to 0,\ \dot{\delta} \to 0,\ \delta \to k\tanh(u_d z_2)$. So (75) can be further simplified as:

$$\dot{V}_4 = -\rho k_u z_1 \tan(z_1) - z_2 u_d \sin[\tanh(u_d z_2)] \tag{79}$$

It is easy to know $\dfrac{\sin[\tanh(u_d z_2)]}{\tanh(u_d z_2)} \in \left(\dfrac{\pi}{2}, 1\right)$, then

$$\dot{V}_4 = -\rho k_u z_1 \tan(z_1) - u_d z_2 \tanh(u_d z_2) \frac{\sin[\tanh(u_d z_2)]}{\tanh(u_d z_2)} \leqslant 0 \tag{80}$$

(3)Case 3: Curve tracking, $r_d \neq 0,\ u_d \neq 0,\ v_d \neq 0$

According to the expression (58) (59), $h \to 0,\ g \to 0$, then (57) can be written as:

$$\ddot{\delta} + 2C_\delta \dot{\delta} + C_\delta^2 \delta = 0 \tag{81}$$

It can be seen from the expression that $\ddot{\delta} \to 0,\ \dot{\delta} \to 0,\ \delta \to 0$, so (75) can be simplified as:

$$\dot{V}_4 = -\rho k_u z_1 \tanh(z_1) \leqslant 0 \tag{82}$$

To sum up, the three cases all satisfy Lyapunov function $\dot{V}_4 \leqslant 0$, so V_4 is bounded, which can approve that $z_1,\ z_2$ is bounded.

The second derivative of $\dot{V}_4$ is easy to know that $\ddot{V}_4$ is bounded, and from the corollary of Barbalat's lemma we know that $\dot{V}_4 \to 0$, thus $z_1 \to 0$.

So, it is easy to know that $\dot{z}_1$ is bounded and z_1 is uniformly continuous. $\dot{z}_1 \to 0$ is inferred from Barbalat's lemma. According to the expression (70) for $\dot{z}_1$, since $r \neq 0$, $z_2 \to 0$.

Substitute (51) and (53) into (50) and it is easy to know that $x_e,\ y_e \to 0,\ u_e,\ v_e \to 0$, that is, both position and velocity errors converge asymptotically to a bounded small domain near zero.

4.3. Proof of saturation input

Firstly, let us think about the boundedness of $u,\ v$.

Construct Lyapunov function:

$$V_{u,v} = \frac{1}{2}\left(cu^2 + \frac{1}{c}v^2\right) \tag{83}$$

The derivation of it is

$$\dot{V}_{u,v} = cu\dot{u} + \frac{1}{c}v\dot{v} = -acu^2 + cu\tau_1 - \frac{1}{b}bv^2 \tag{84}$$

For the convenience of expression, let

$$V_1 = cu^2,\ V_2 = \frac{1}{c}v^2,\ m_{ab} = \min(a,b) \tag{85}$$

Equation (84) can be written as:

$$\dot{V}_{u,v} \leqslant m_{ab}(V_1 + V_2) + cu\tau_1 = -2m_{ab}\left(V - \frac{cu\tau_1}{2m_{ab}}\right) \tag{86}$$

According to the formula above, $\dot{V}_{u,v} \leqslant 0$ if $V_{u,v} \geqslant \frac{cu\tau_1}{2m_{ab}}$.

$V_{u,v}$ is analyzed as follows:

(1) $V_{u,v} \leqslant \frac{cu\tau_1}{2m_{ab}}$, the function $V_{u,v}$ has an upper bound $\frac{cu\tau_{1,\max}}{2m_{ab}}$;

(2) When $V_{u,v} \geqslant \frac{cu\tau_1}{2m_{ab}}$, $\dot{V}_{u,v} \leqslant 0$, the inequality can be written as:

$$\dot{V}_{u,v}(t) = -\varepsilon \tag{87}$$

Where ε is a positive small quantity.

So, the integral of equation (87) is

$$V(t) - V(0) = -\varepsilon t \tag{88}$$

Let $V(T) = 0$ at time T,then

$$T = \frac{V(0)}{\varepsilon} \tag{89}$$

As can be seen from the above formula, T is a bounded value.

Therefore, it can be proved that when $V_{u,v} \geqslant \frac{cu\tau_1}{2m_{ab}}$; the system is stabilized in a finite time, that is, when $t > T = \frac{V(0)}{\varepsilon}$; $\dot{V}_{u,v} < 0$ and the system will eventually converge to $V(t) \leqslant \frac{cu\tau_1}{2m_{ab}}$.

To sum up, the following conclusions can be drawn:

$$\lim_{t\to\infty} sup V(t) \leqslant \frac{cu\tau_{1,\max}}{2m_{ab}} \tag{90}$$

By the definition of V_1, V_2, $V_{u,v}$, there is

$$\frac{1}{2}V_1 \leqslant V_{u,v} \tag{91}$$

Substitute it into equation (90), we can get

$$\lim_{t\to\infty} sup\,\frac{1}{2}V_1 \leqslant \frac{cu\tau_{1,\max}}{2m_{ab}} \tag{92}$$

Then substitute it into equation (85), it is can be obtained that

$$\lim_{t\to\infty} sup\,|u| \leqslant \sqrt{\frac{c\tau_{1,\max}}{m_{ab}}} \tag{93}$$

In the same way, the supremum of v can be obtained:

$$\lim_{t\to\infty} sup\,|v| = c\sqrt{\frac{(\tau_{1,\max})^{\frac{3}{2}}\sqrt{c}}{(m_{ab})^{\frac{3}{2}}}} \tag{94}$$

Observe the control input $\tau_1,\ \tau_2$ designed above:

$$\tau_1 = \dot{u}_d + au_d + \frac{-r_d + \dot{\delta}}{c}v_d - \frac{f_1(\delta) + (1-a\rho)u_e}{\rho} - k_u\tanh(z_1)$$

$$\tau_2 = -\kappa uv + \dot{r}_d - \ddot{\delta} + d\left(r_d - \dot{\delta}\right) - k_r\tanh\left(\bar{r}_e + \bar{\psi}_e\right)$$

From the above analysis, we can see that $\dot{\delta},\ \ddot{\delta}$ approaches 0 with time, and $f_1(\delta),\ \tanh(\cdot)$ themselves are bounded function, so by selecting appropriate parameters $a,\ c,\ \rho,\ d,\ k_u.\ k_r$ and desired velocitiy $u_d,\ \dot{u}_d,\ r_d,\ \dot{r}_d$, we can obtain bounded control input to meet the saturation input limit, that is:

$$|\tau_1| \leqslant \tau_{1,\max} \leqslant \bar{\tau}_{1,\max} \tag{95}$$

$$|\tau_2| \leqslant \tau_{2,\max} \leqslant \bar{\tau}_{2,\max} \tag{96}$$

Where $\bar{\tau}_{1,\max},\ \bar{\tau}_{2,\max}$ is the maximum output of the actuators of AUV respectively.

4.4. Simulation and analysis

In order to verify the effectiveness of the control method designed in this thesis, this section verifies the control effect of AUV two-dimensional simultaneous tracking and stabilization by using the Simulink module in MATLAB.

According to the physical model parameters used by Do, Jiang and Pan (Do et al., 2002), it is assumed that the roll, pitch and heave motion of AUV and the effects of nonlinear damping terms can be ignored. The model parameters of AUV are as follows:

$$m_{11} = 120 \times 10^3 kg,\ m_{22} = 172.9 \times 10^3 kg,\ m_{33} = 636 \times 10^5 kg$$
$$d_{11} = 215 \times 10^2 kg \cdot s^{-1},\ d_{22} = 97 \times 10^3 kg \cdot s^{-1},\ d_{33} = 636 \times 10^5 kg \cdot s^{-1}$$

Substitute them into the AUV physical model mentioned before, and the parameters of the system are:

$$a = 0.179,\ b = 0.561,\ c = 0.604,\ d = 0.126$$
$$\kappa = -8.32 \times e^{-4},\ \rho = c/b = 1.07665$$

The initial state of AUV is set to: $x(0) = 15m,\ y(0) = 15m,\ \psi(0) = 0.7rad$

The maximum value of the control input is set to: $\bar{\tau}_{1,\max} = 6,\ \bar{\tau}_{2,\max} = 3$

When tracking, the reference velocity is selected as follows: $u_d = 1.0m/s,\ r_d = 0.02rad/s$

In order to achieve better control performance, the control parameters are set to:

$k_r = 0.5,\ k_u = 5,\ k_\delta = 1.8,\ C_\delta = 2,\ k_h = 50,\ k_g = 2$

The Simulink block diagram is as follows.

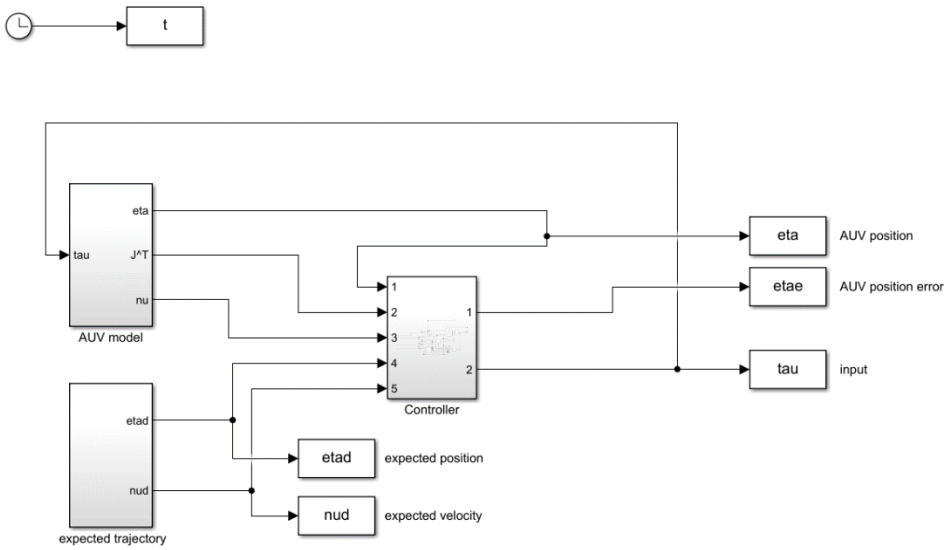

Figure 7. Simulink block diagram - single AUV

4.4.1. Simulation of point stabilization control

First of all, the stabilization problem is simulated, $u_d = 0m/s,\ r_d = 0rad/s$, and the position and attitude of the stabilization point is $x_d = 0.5m,\ y_d = 0.5m,\ \psi_d = 0.2rad$. The simulation time is 400s.

The simulation results are as follows:

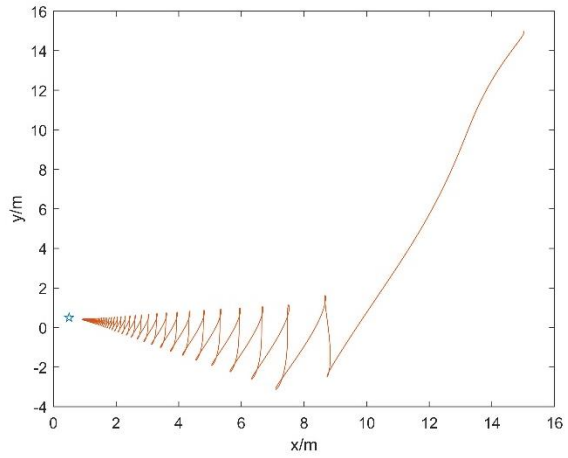

(a) Stabilization trajectory of AUV

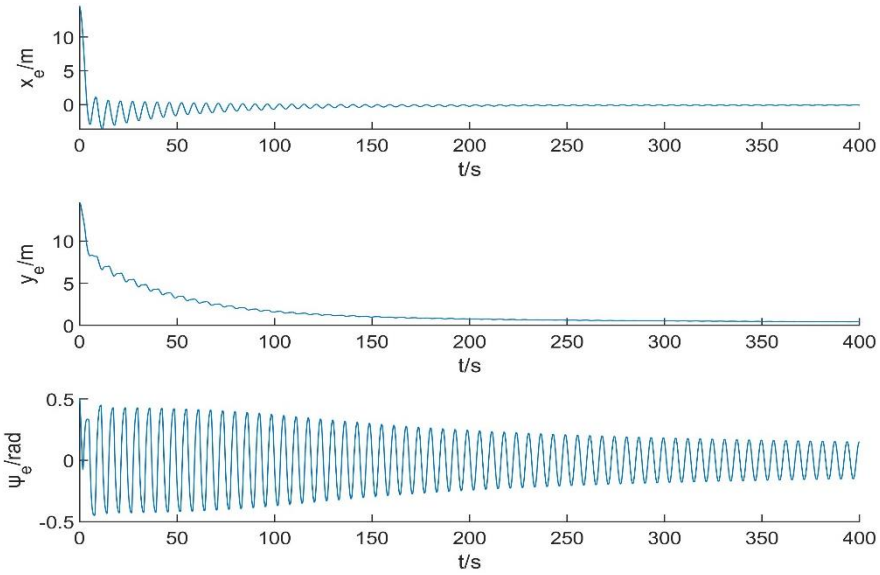

(b) Stabilization errors

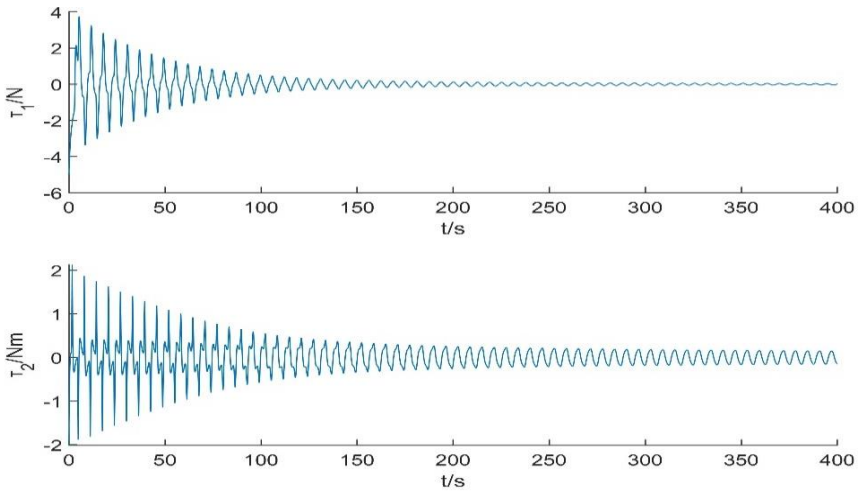

(c) Control inputs

Figure 8. Simulation results of AUV stabilization control in 2-Dimension

It can be seen from Figure 8 that without environmental interference, the controller designed in this thesis can drive the AUV to reach a small error range near the specified position and attitude within a certain period of time and maintain it. Although the chattering in the stabilization process is inevitable, the error still converges gradually with time. In the stabilization process, the control input does not exceed the maximum value that the actuator can provide, and gradually converge to a small fluctuation near zero. The requirement of stabilization control can be achieved.

4.4.2. Simulation of trajectory tracking Control

Next, the tracking problem is simulated, and the simulation time is 400s. In this paper, the first 100s is set as linear trajectory tracking, with velocity of $u_d = 1m/s,\ r_d = 0rad/s$. The last 300s is curve (circle) trajectory tracking, with velocity of $u_d = 1m/s,\ r_d = 0.02rad/s$.

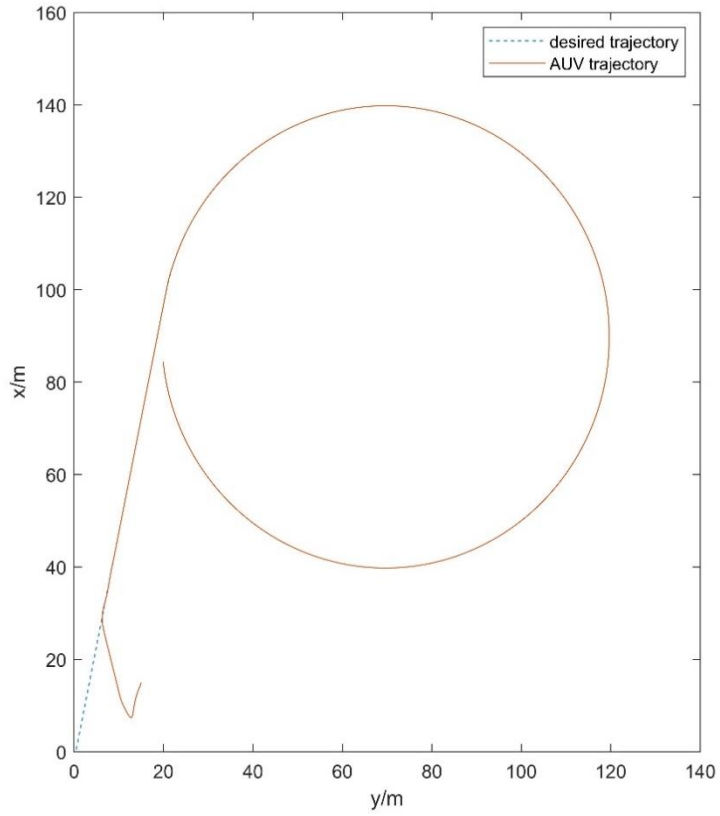

(a) Tracking trajectory of AUV

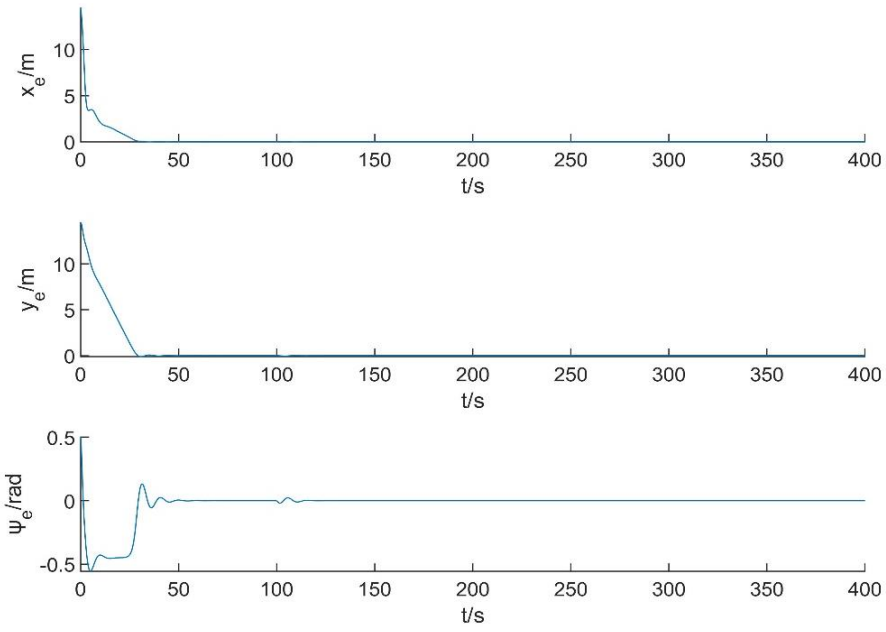

(b) Tracking errors

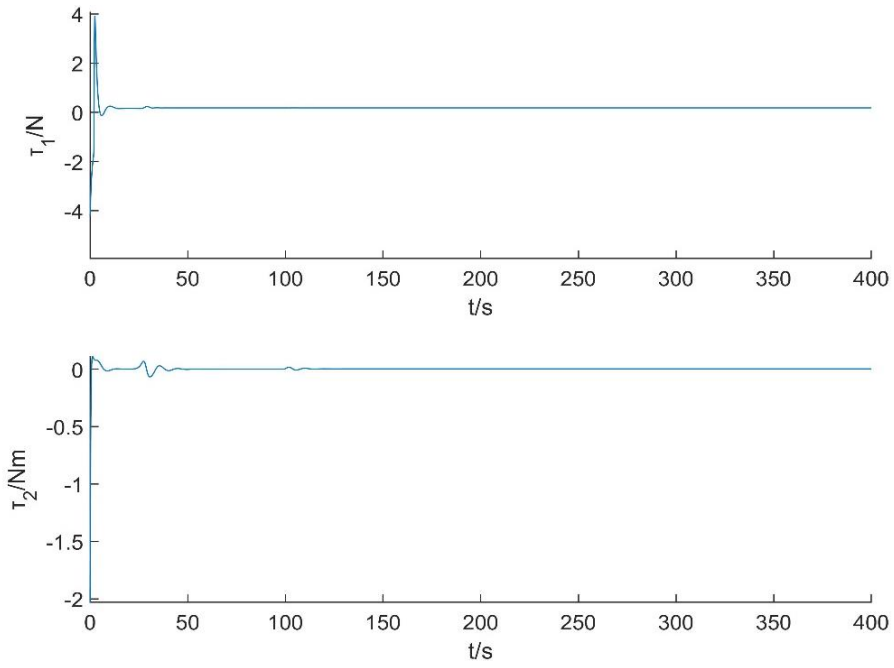

(c) Control inputs

Figure 9. Simulation results of AUV trajectory tracking control in 2-Dimension

As shown in Figure 9, AUV can quickly track the desired trajectory under the action of the controller designed above. The motion curve is smooth, and the tracking error converges to a bounded small domain near the zero point. The control input does not exceed the maximum value that the actuator can provide. The control target of trajectory tracking can be achieved.

4.5. Event triggered control of underactuated AUV

In this section, we use the controller designed in the previous section, and design the event trigger mechanism and event trigger controller on this basis, so as to reduce the actuator driving frequency and consumption.

4.5.1. Event triggered controller (ETC) design

Sampling error is defined as $\Delta_i = \tau_i(t) - \hat{\tau}_i(t)$, $i = 1, 2$, where $\tau_i(t)$ is the continuous control signal calculated by the controller designed above according to AUV state at time t, and $\hat{\tau}_i(t)$ is the actual control input of AUV.

In this thesis, the proportional threshold is adopted, and the event triggering conditions are designed as follows:

$$\begin{aligned} &\hat{\tau}_i(t) = \tau_i(t_k), \quad t \in [t_{i,k}, t_{i,k+1}) \\ &t_{i,k+1} = inf\{\Delta_i \geq C_i|\hat{\tau}_i| + D_i\} \end{aligned} \tag{97}$$

Where $k = 1, 2, 3\cdots, t_{i,0} = 0$ and $C_i,\ D_i (i = 1, 2)$ are suitable positive constants.

The trigger mechanism represented by formula (97) is described as follows: ETC samples the computational control signal $\tau_i(t)$ at trigger time $t_{i,k}$:$\hat{\tau}_i(t) = \tau_i(t_{i,k})$. The propeller of AUV executes it as the actual control input and remains unchanged in time period $t \in [t_{i,k}, t_{i,k+1})$. When the sampling error Δ_i meets the triggering condition (97) again, the triggering moment $t_{i,k+1}$ is recorded, and $\tau_i(t)$ is sampled again, and the actual control input is updated as $\hat{\tau}_i(t) = \tau_i(t_{i,k+1})$ and kept until the next triggering moment $t_{i,k+2}$.....

The stability analysis is the following:

According to Formula (97), there exist functions $\lambda_{i1}(t)$ and $\lambda_{i2}(t)$ that satisfy $|\lambda_{i1}(t)|, |\lambda_{i2}(t)| \leqslant 1$, so that $\tau_i(t) = (1 + \lambda_{i1}(t)C_i)\hat{\tau}_i(t) + \lambda_{i2}(t)D_i$, that is

$$\hat{\tau}_i(t) = \frac{\tau_i(t) - \lambda_{i2}(t)D_i}{1 + \lambda_{i1}(t)C_i} = \frac{1}{1 + \lambda_{i1}(t)C_i}\tau_{i,ETC}(t) - \frac{\lambda_{i2}(t)D_i}{1 + \lambda_{i1}(t)C_i} \tag{98}$$

According to Equation (52), the controller based on event triggering is designed as follows:

$$\begin{aligned} \tau_{1,ETC} &= D_1 \mathrm{sgn}(u_e) - k_1 \tanh(u_e) - F_u - |\lambda_{11}|_{\max}|F_u|C_1 \mathrm{sgn}(u_e) \\ \tau_{2,ETC} &= D_2 \mathrm{sgn}(r_e) - k_2 \tanh(r_e) - F_r - |\lambda_{21}|_{\max}|F_r|C_2 \mathrm{sgn}(r_e) \end{aligned} \tag{99}$$

Where:

$$F_u = \dot{u}_e - \tau_1 = \frac{r}{c} v_e - a u_e - \dot{u}_d + \frac{r}{c} v_d - a u_d$$
$$F_r = \dot{r}_e - \tau_2 = \kappa u v - d r - r_d \tag{100}$$

According to the definition above, $|\lambda_{11}(t)|_{\max}$, $|\lambda_{12}(t)|_{\max}$, $|\lambda_{21}(t)|_{\max}$, $|\lambda_{22}(t)|_{\max} \leq 1$

Substitute Equation (99) (98) into equation (52), then:

$$\begin{aligned}
\dot{u}_e &= F_u + \hat{\tau}_1 \\
&= F_u + \frac{1}{1+\lambda_{11}(t) C_1} \left[D_1 \operatorname{sgn}(u_e) - k_1 \tanh(u_e) - F_u - |\lambda_{11}|_{\max} |F_u| C_1 \operatorname{sgn}(u_e) \right] - \frac{\lambda_{12}(t) D_1}{1+\lambda_{11} C_1} \\
\dot{r}_e &= F_r + \hat{\tau}_2 \\
&= F_r + \frac{1}{1+\lambda_{21}(t) C_2} \left[D_2 \operatorname{sgn}(r_e) - k_2 \tanh(r_e) - F_r - |\lambda_{21}|_{\max} |F_r| C_2 \operatorname{sgn}(r_e) \right] - \frac{\lambda_{22}(t) D_2}{1+\lambda_{21} C_2}
\end{aligned} \tag{101}$$

Design the Lyapunov function:

$$V_{u,ETC} = \frac{1}{2} u_e^2, \; V_{r,ETC} = \frac{1}{2} r_e^2 \tag{102}$$

The derivative of the Lyapunov function with respect to time is as follows:

$$\dot{V}_{u,ETC} = u_e \dot{u}_e, \; \dot{V}_{r,ETC} = r_e \dot{r}_e \tag{103}$$

Substitute into equation (101), it is easy to know:

$$\dot{V}_{u,ETC} \leq 0, \; \dot{V}_{r,ETC} \leq 0 \tag{104}$$

Therefore, under the control of the ETC, the velocity error of the system will be gradually stable, indicating that the ETEC has no influence on the stability of the system.

4.5.2. Zeno behavior analysis

Zeno behavior refers to the phenomenon of triggering an infinite number of times in a finite period of time in event triggering control. This phenomenon is not reasonable in reality, but also physically possible.

However, event triggering control design is a mathematical process, so in the process of setting event triggering conditions, it is necessary to avoid conflicts with physical implementation and analyze whether Zeno behavior exists.

In this thesis, the positive lower bound (Fan, Feng, Wang & Song, 2013) method is used for Zeno analysis: If any two trigger intervals have a positive minimum value during the control process, Zeno behavior can be guaranteed to be excluded.

Taking the derivative of Equation (72) (62), it can be analyzed that, for $\dot{\tau}_1$, $\dot{\tau}_2$, there is a bounded maximum value $0 < \dot{\tau}_{1,\max}$, $\dot{\tau}_{2,\max} < +\infty$.

Taking the derivative of sampling error $\Delta_i = \tau_i(t) - \hat{\tau}_i(t)$, $\hat{\tau}_i(t)$ does not change in the two nearest trigger intervals, so:

$$\dot{\Delta}_i = \dot{\tau}_i(t) \tag{105}$$

Considering that there is a maximum value of $\dot{\tau}_i(t)$, then:

$$\left|\dot{\Delta}_i\right| = |\dot{\tau}_i| \leqslant \tau_{i,\max} \tag{106}$$

According to formula (97), it is easy to know that

$$\begin{aligned} &\lim_{t \to t_{i,k}} |\Delta_i| = 0 \\ &\lim_{t \to t_{i,k+1}^-} |\Delta_i| = C_i |\hat{\tau}_i(t)| + D_i \end{aligned} \tag{107}$$

Take equation (106) and (107) in to consideration, it can be seen that the lower bound of triggering interval $\Delta T = t_{i,k+1}^- - t_{i,k}$ must satisfy:

$$inf(\Delta T)\dot{\tau}_{i,\max} \geqslant \min\{|\Delta_i|\} \tag{108}$$

That is

$$\Delta T \geqslant \frac{C_i |\tau_i(t)| + D_i}{\dot{\tau}_{i,\max}} > 0 \tag{109}$$

Thus, it can be proved that the minimum triggering interval of the ETC designed in this thesis must be positive, thus proving that Zeno phenomenon will not occur.

4.5.3. Simulation and analysis

AUV model parameters used in this section are the same as those in the previous section.

The parameters of the event trigger are designed as follows:

$C_1 = 0.1,\ D_1 = 0.003;\ C_2 = 0.1,\ D_2 = 0.003$

The Simulink block diagram is as follows.

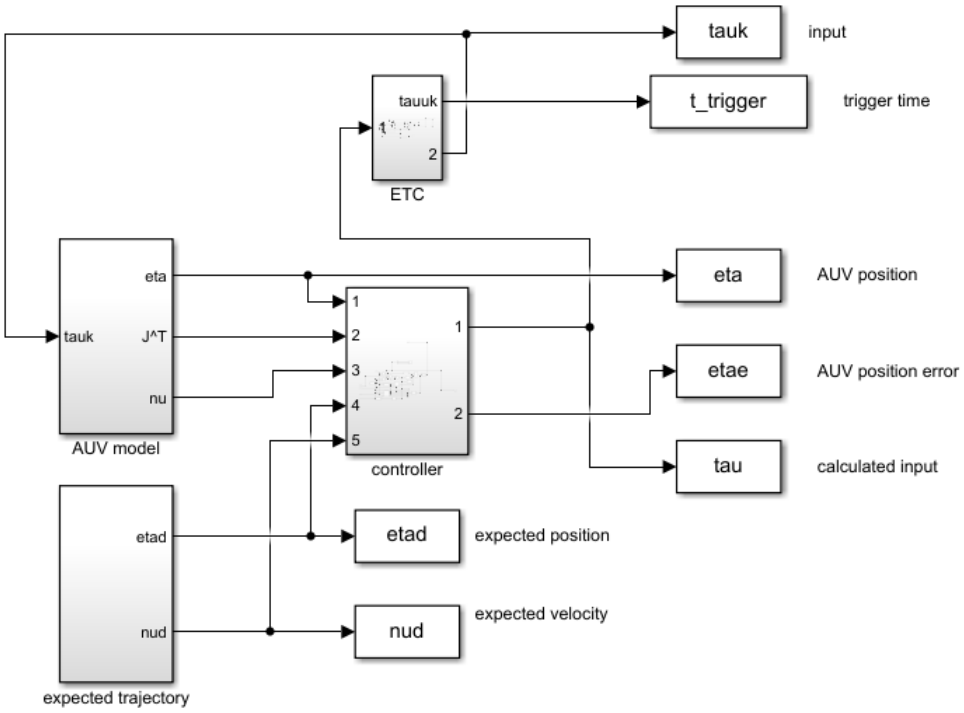

Figure 10. Simulink block diagram - single AUV with ETC

4.5.3.1. Simulation of Point stabilization event trigger control

Firstly, the stabilization problem is simulated. The position and attitude of the stabilized target is $x_d = 0.5m,\ y_d = 0.5m,\ \psi_d = 0.2rad$, $u_d = 0m/s,\ r_d = 0rad/s$, and the simulation time is 400 seconds.

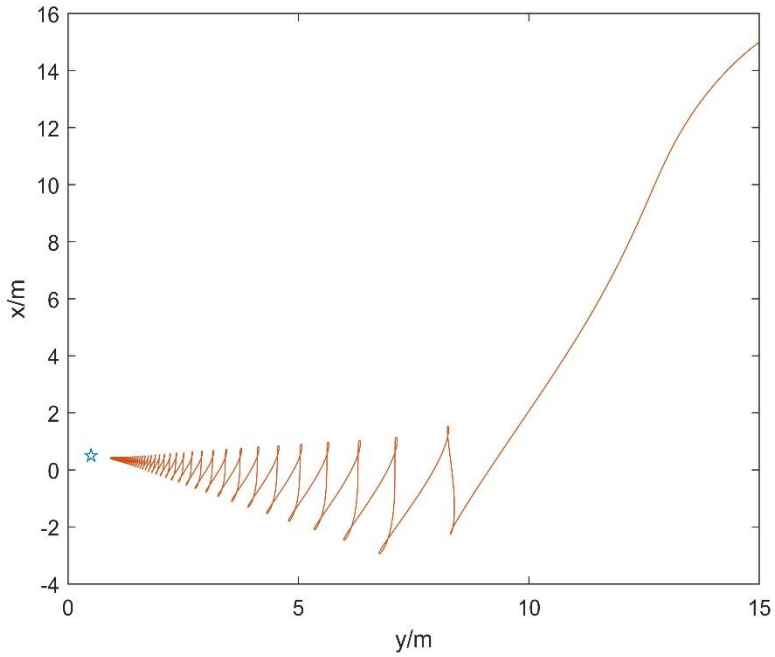

(a) ETC-based stabilization trajectory

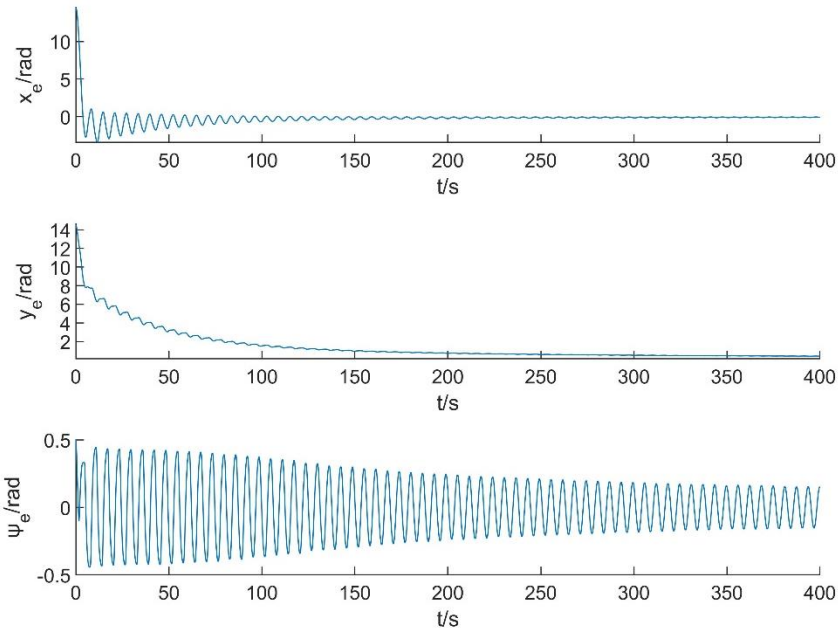

(b) ETC-based stabilization errors

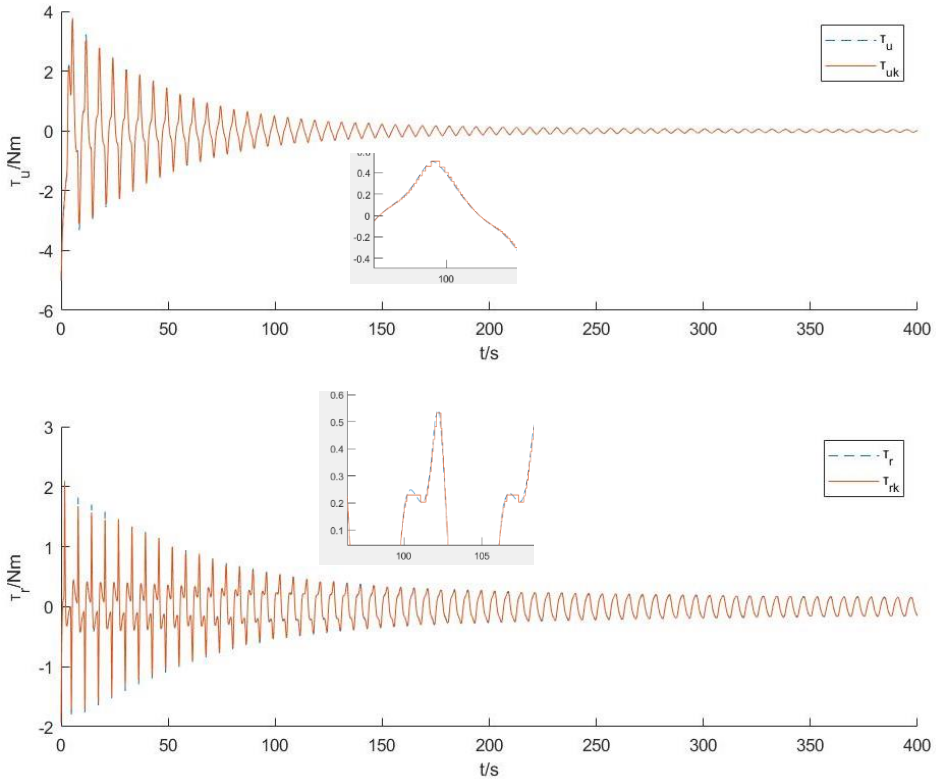

(c) Control inputs comparison (actual input & signal input)

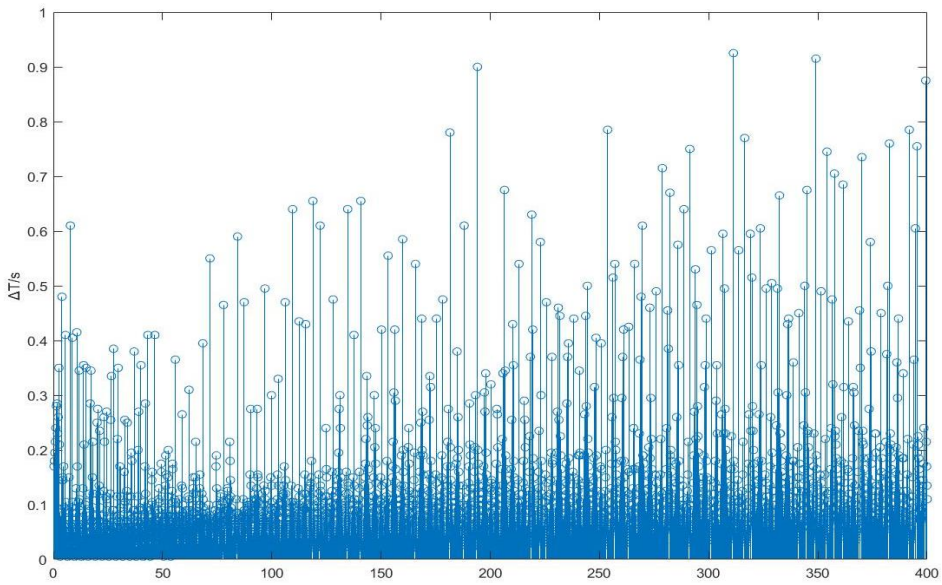

(d) Triggered span of τ_u

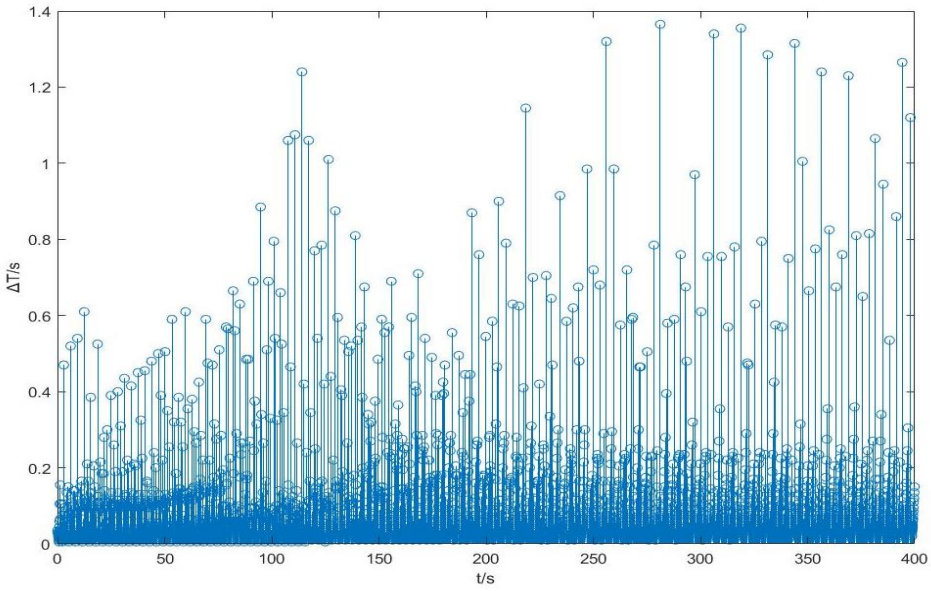

(e) Triggered span of τ_r

Figure 11. Simulation results of ETC-based AUV stabilization control in 2-Dimension

As can be seen from Figure 11, in the stabilization control, the introduction of ETC has no obvious influence on the control result and control efficiency of the original controller.

According to the statistics of simulation results, the number of trigger sampling of τ_u is 5181 times, and the number of trigger sampling of τ_r is 6129 times. The actuator that does not need AUV keeps working at all times.

4.5.3.2. Simulation of trajectory tracking event trigger control

Next, the trajectory tracking problem is simulated. A 400s simulation duration is set in this paper. The first 100s is linear trajectory tracking: $u_d = 1m/s,\ r_d = 0rad/s$, and the last 300s is curve track tracking: $u_d = 1m/s,\ r_d = 0.02rad/s$.

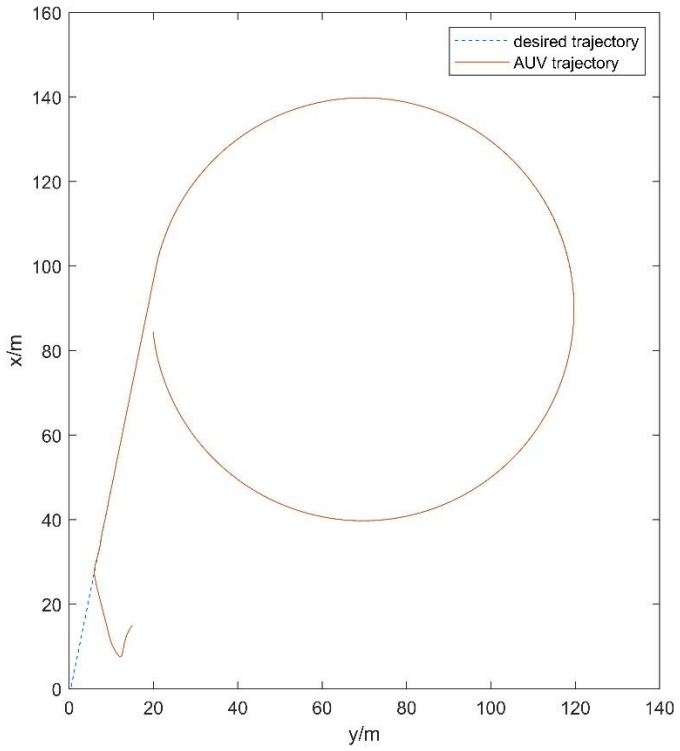

(a) Tracking trajectory of AUV

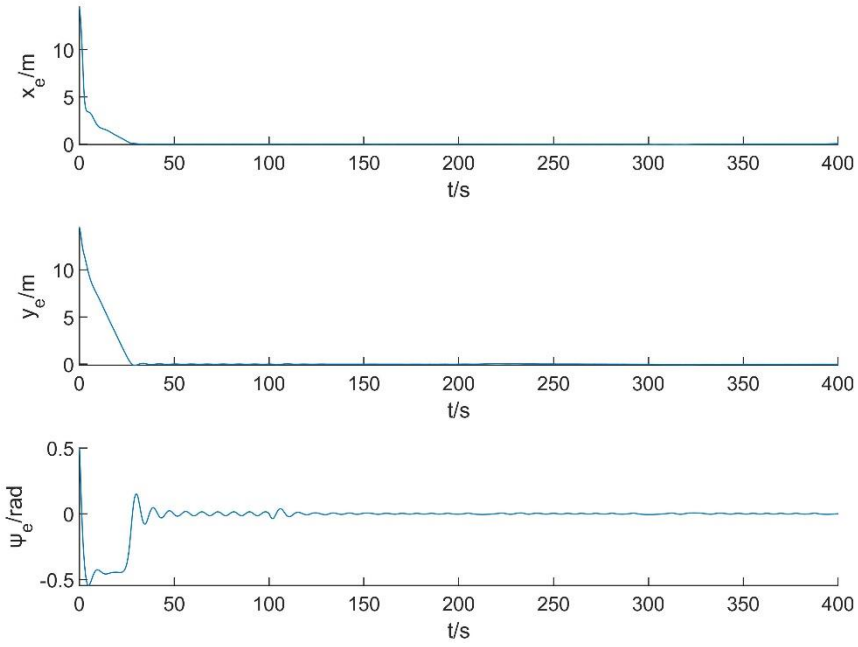

(b) Tracking errors

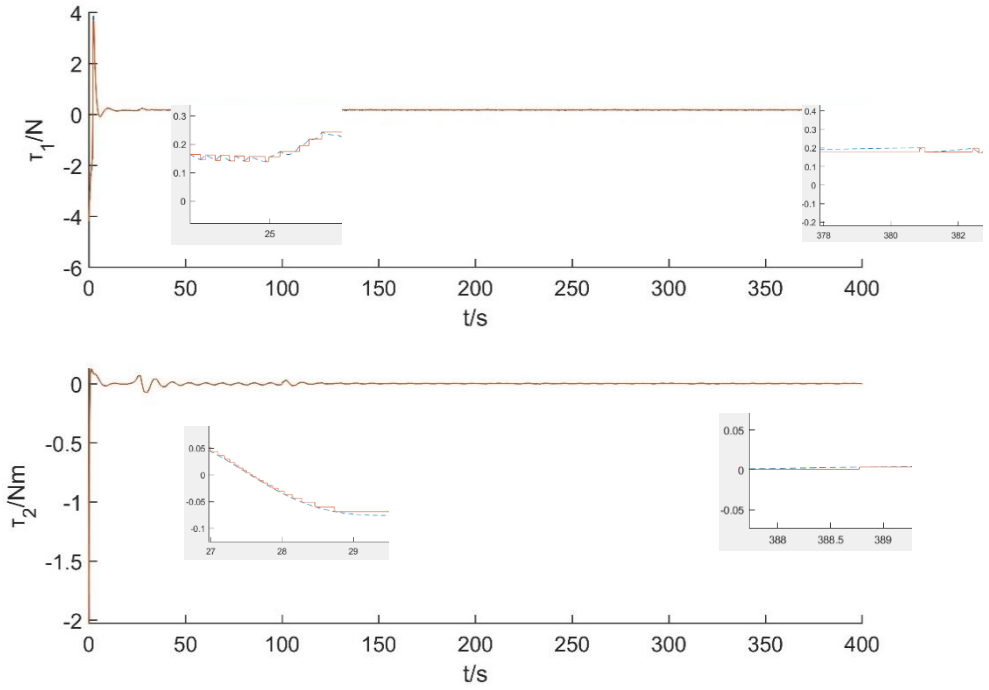

(c) Control inputs

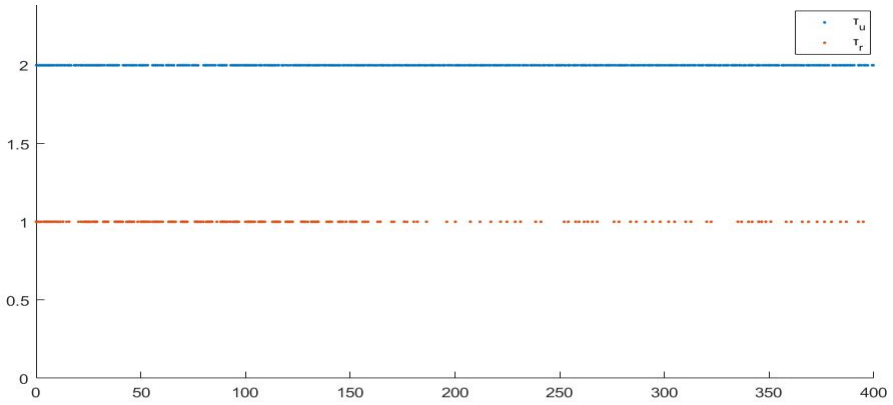

(d) Trigger time

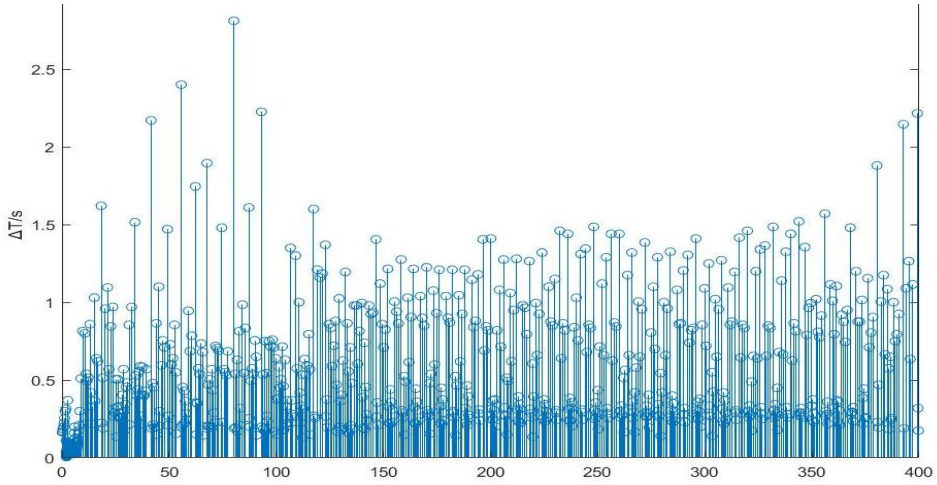

(e) Trigger span of τ_u

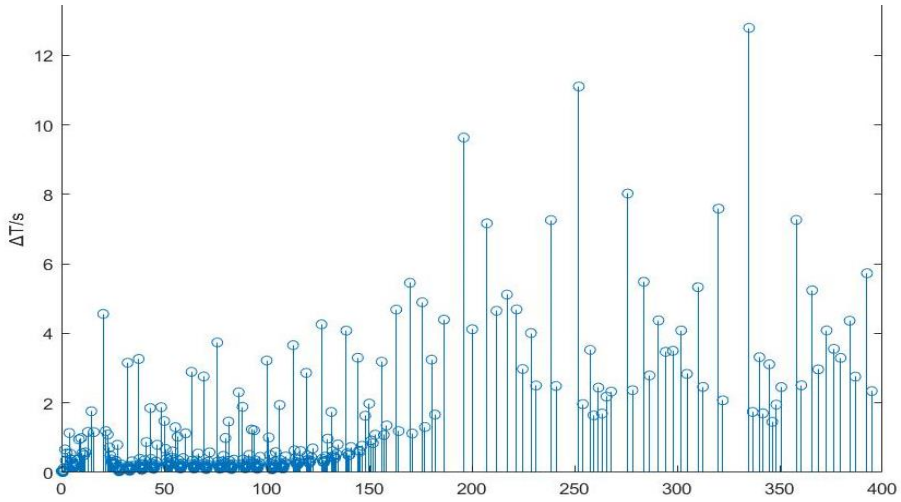

(f) Trigger span of τ_r

Figure 12. Simulation results of ETC-based AUV trajectory tracking control in 2-Dimension

As it can be seen from Figure 12, in the control of trajectory tracking, the introduction of ETC has no obvious influence on the control results and control efficiency of the original controller. The tracking trajectory of AUV is still smooth and the tracking error converges rapidly.

According to the statistics of simulation results, the trigger sampling times of τ_u is 774 times, and the trigger sampling times of τ_r is 454 times, indicating a significant decrease in the trigger frequency. Especially in the process of circular trajectory tracking, the maximum departure interval of τ_r can reach 12.79s, which can greatly reduce the consumption of AUV power actuator in practice.

Chapter 5. Results - Underactuated AUV formation tracking control

In chapter 4, a controller based on event triggering mechanism is designed for a single underactuated AUV, which solves the problems of simultaneous tracking and stabilization control of AUV with limited control input.

In the control process of multi-AUV formation, communication between AUVs is always in a restricted state due to the complex and harsh ocean environment. How to occupy the least communication resources to transmit information between individuals in the formation has become the key to solve the problem.

Chapter 5 first combines the idea of line-of-sight (LOS) method and virtual structure method, and calculates the desired trajectory that the follower needs to track according to the real-time information of the leader. Then, aiming at the communication limitation, an ETC with the leader state as the trigger condition is designed to be triggered only when necessary to reduce the communication times. Finally, the effectiveness of the formation control method is verified by numerical simulation.

This chapter will study the control of a formation containing three AUVs. Based on the controller designed in the previous chapter, the follower is controlled to keep its position in the leader's body-fixed frame, and the desired angle should fit the formation. To track the trajectory as a whole and maintain the formation.

5.1. The transformation between the follower's desired position and attitude with kinematics equation

In formation, the information sent by the leader to the followers includes its position, yaw angle, longitudinal velocity and yaw velocity. Among them the position and yaw angle are based on the

earth-fixed frame, while the follower needs to carry out coordinate transformation in order to achieve the goal of unchanged desired position in the leader's body-fixed frame.

5.1.1. The desired position of the follower

The coordinate of the leader in the earth-fixed frame is defined as (x_l, y_l, ψ_l), the coordinate of the follower in the leader's body-fixed frame is defined as $(x_{f,i}, y_{f,i}, \psi_{f,i})$, and the coordinate of the follower in the earth-fixed frame is defined as (L_x, L_y, L_ψ). The three can be converted through matrix change below:

$$\begin{bmatrix} -L_x \\ L_y \end{bmatrix} = \begin{bmatrix} \cos\psi_l & \sin\psi_l \\ \sin\psi_l & -\cos\psi_l \end{bmatrix} \begin{bmatrix} x_l - x_f \\ y_l - u_f \end{bmatrix} \tag{110}$$

$$\begin{bmatrix} x_f \\ y_f \end{bmatrix} = \begin{bmatrix} x_l \\ y_l \end{bmatrix} - \begin{bmatrix} \cos\psi_l & \sin\psi_l \\ \sin\psi_l & -\cos\psi_l \end{bmatrix} \begin{bmatrix} -L_x \\ L_y \end{bmatrix} \tag{111}$$

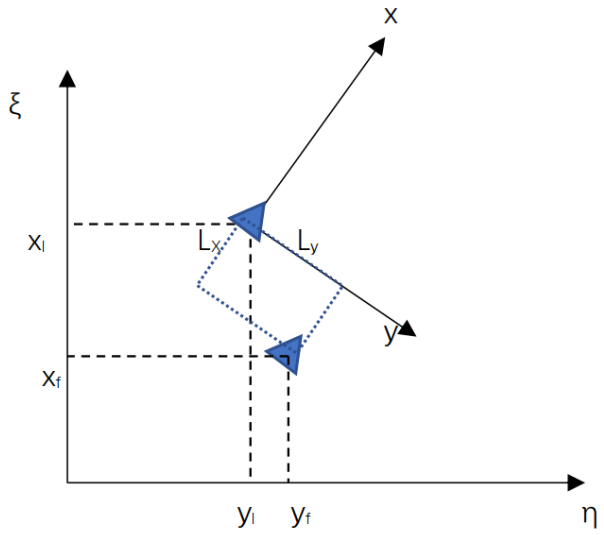

Figure 13. Coordinate transformation

Before starting work, the coordinate of the follower in the leader's body-fixed frame has been given, denoted as $(L_{xd}, L_{yd}, L_{\psi d})$. Through communication equipment, the follower can obtain the coordinate (x_l, y_l, ψ_l) of the leader in the earth-fixed frame. According to Equation (111), the follower's desired coordinate $(x_{fd}, y_{fd}, \psi_{fd})$ in the earth-fixed frame can be obtained:

$$\begin{bmatrix} x_{fd} \\ y_{fd} \end{bmatrix} = \begin{bmatrix} x_l \\ y_l \end{bmatrix} - \begin{bmatrix} \cos\psi_l & \sin\psi_l \\ \sin\psi_l & -\cos\psi_l \end{bmatrix} \begin{bmatrix} -L_{xd} \\ L_{yd} \end{bmatrix} \tag{112}$$

5.1.2. The desired angle of the follower

Due to the underdrive limitation of AUV, it is not possible to directly make $\psi_{fd} = \psi_l$, so the LOS method is used here to adjust the yaw angle of the followers

The basic idea of line-of-sight method is as follows: Based on the projection on the x-axis and y-axis of the deviation between the desired position and the actual position of the follower in the leader's body-fixed frame, the deviation in the x-axis direction is used to control the ship longitudinal velocity, and the deviation in the y-axis direction is used to control the yaw angle, so as to form the desired path and realize the desired formation.

Its advantage lies in that it does not need to rely on the model of the controlled object, and the controller can be designed in the case of uncertain parameters or external disturbances to realize the control of the system (Borhaug, Pavlov & Pettersen, 2008).

In this thesis, we only use the error in the y-axis direction to flexibly adjust the yaw angle, so that the follower gradually approaches the desired position before reaching the desired position, and keeps the desired position and consistent with the yaw angle of the leader when reaching the desired position.

In the leader's body-fixed frame, defined the errors between the follower's actual coordinate and the desired coordinate are:

$$\begin{aligned} e_x &= L_x - L_{xd} \\ e_y &= L_y - L_{yd} \end{aligned} \tag{113}$$

Combining formula (110), there is

$$\begin{bmatrix} e_x \\ e_y \end{bmatrix} = \begin{bmatrix} L_x - L_{xd} \\ L_y - L_{yd} \end{bmatrix} = \begin{bmatrix} -\cos\psi_l & -\sin\psi_l \\ \sin\psi_l & -\cos\psi_l \end{bmatrix} \begin{bmatrix} x_l - x_f \\ y_l - y_f \end{bmatrix} - \begin{bmatrix} L_{xd} \\ L_{yd} \end{bmatrix} \tag{114}$$

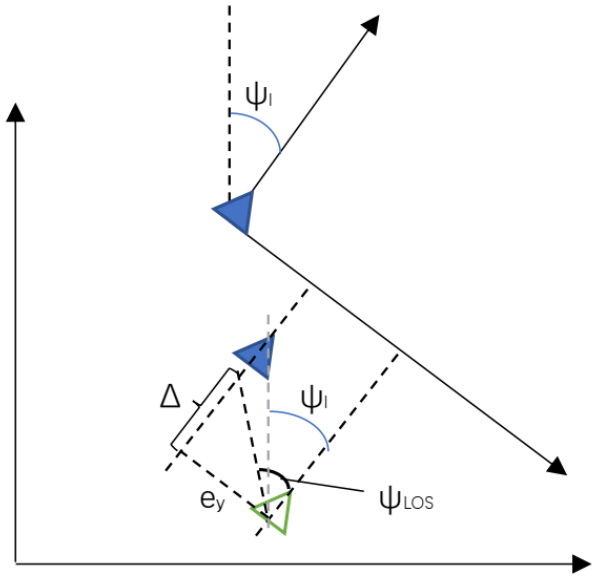

Figure 14. Light-of-sight method

The desired yaw angle of the follower is expressed as follows:

$$\psi_{fd} = \psi_l - \psi_{LOS} \tag{115}$$

Which ψ_{LOS} is the line-of-sight angle, defined as follows: at the follower's desired position, a straight line is drawn along the leader's heading. Project the actual position of the follower on the straight line, mark a point in front of the subpoint and the distance between them is Δ ($\Delta > 0$). Draw a line from the current position of the follower to this point, the angle between the direction of this line and the leader's heading, is the line-of-sight angle.

By definition, we have the expression ψ_{LOS}:

$$\psi_{LOS} = \arctan \frac{e_y}{\Delta} \tag{116}$$

Where $\Delta = k_{\Delta 1} + k_{\Delta 2}\mathrm{sgn}(e_x - e_y)$, $k_{\Delta 1}$, $k_{\Delta 2}$ is the given constant.

Here, Δ adopts an improved parameter whose expression includes e_x and e_y at the same time, which means that the parameter Δ can be adjusted automatically according to e_x and e_y, making the adjustment of yaw angle more suitable for different situations in the formation tracking process.

So far, the follower's desired position and attitude in the earth-fixed frame can be obtained:

$$\begin{bmatrix} x_{fd} \\ y_{fd} \end{bmatrix} = \begin{bmatrix} x_l \\ y_l \end{bmatrix} - \begin{bmatrix} \cos\psi_l & \sin\psi_l \\ \sin\psi_l & -\cos\psi_l \end{bmatrix} \begin{bmatrix} -L_{xd} \\ L_{yd} \end{bmatrix} \tag{117}$$
$$\psi_d = \psi_l - \psi_{LOS}$$

5.1.3. The desired velocity of the follower

For the desired velocity of the follower (u_{fd}, v_{fd}, r_{fd}), the idea of virtual structure is introduced in this thesis, and the instantaneous desired configuration of AUV formation is analyzed as rigid body.

It is noted that the velocity of the leader in the earth-fixed frame is (u_l, v_l, r_l), which satisfies the kinematics and dynamics equations (38) and (39) in Chapter 3.

When the formation is tracking the circular trajectory, the desired velocity of the follower can be regarded as the plane motion of the "virtual rigid body" by using the idea of theoretical mechanics. The motion can be divided into the circular motion of the leader's center of gravity and the circular motion of the follower's center of gravity with the leader's center of gravity as the center of the circle.

According to the synthesis of motion, there are:

$$\boldsymbol{u}_{fd} = \boldsymbol{u}_l + \boldsymbol{u}_{lfd} \tag{118}$$

Where $\boldsymbol{u}_{fd}$ is the desired combined velocity of the follower in the earth-fixed frame, $\boldsymbol{u}_l$ is the combined velocity of the leader in the earth-fixed frame, $\boldsymbol{u}_{lfd}$ is the desired relative velocity of the leader and the follower, and its magnitude is $|\boldsymbol{v}_{lf}| = r_l \cdot LF$, where LF is the distance between the leader and the follower.

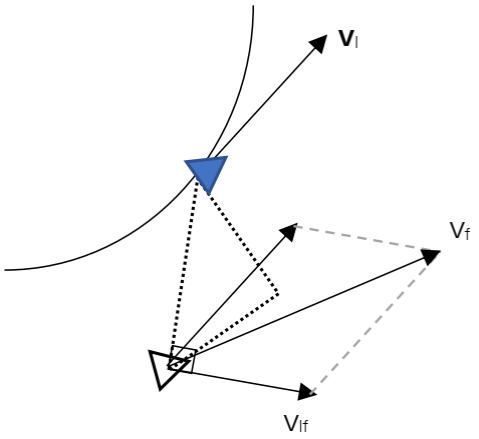

Figure 15. Velocity combination

According to the graph of velocity combination, there are:

$$u_{fd} = |\boldsymbol{u}_{fd}| = \sqrt{v_l^2 + u_l^2 + r_l^2 (L_x + L_y)^2 - v_f^2} \tag{119}$$

For angular velocity, the angular velocity of each point of "virtual rigid body" is equal:

$$r_{fd} = r_l \tag{120}$$

When the formation tracks the straight track, it can be regarded as the "virtual rigid body" moving in parallel, and the desired speed of the follower is completely same as that of the leader: $r_{fd} = r_l = 0,\ u_f = u_l$, which can be regarded as the special case of Equation (119).

v_{fd} can be calculated from u_{fd} and r_{fd} according to the mathematical model:

$\dot{v}_{fd} = -cu_{fd}r_{fd} - bv_{fd}$

5.2. AUV formation tracking control

5.2.1. Controller design

The basic idea of formation control in this chapter is as follows: the desired trajectory and formation shape of the leader are given; the leader uses the controller designed in Chapter 4 to track the desired trajectory. At the same time, the followers received the leader's status information which includes position, yaw angle and velocity through the receiver. The followers calculate their own desired trajectory to be track by the method of follower's desired position, attitude and velocity, which is introduced in 5.1. Then they control themselves to track their own

trajectory respectively using the controller designed in Chapter 4, so as to achieve the effect of formation control as a whole.

By combining the formulae (117) (119) (120), the desired trajectory of the follower can be obtained:

$$\begin{bmatrix} x_{fid} \\ y_{fid} \end{bmatrix} = \begin{bmatrix} x_l \\ y_l \end{bmatrix} - \begin{bmatrix} \cos\psi_l & \sin\psi_l \\ \sin\psi_l & -\cos\psi_l \end{bmatrix} \begin{bmatrix} L_{xid} \\ L_{yid} \end{bmatrix} \tag{121}$$

$$\psi_{fid} = \psi_l - \arctan\frac{e_{yi}}{k_{\Delta 1i} + k_{\Delta 2i}\,\mathrm{sgn}\,(e_{xi} - e_{yi})}$$

$$\begin{cases} u_{fid} = \sqrt{{v_l}^2 + {u_l}^2 + r_l^2 (L_x^2 + L_y^2) - v_f^2} \\ \dot{v}_{fid} = -cu_{fid} r_{fid} - bv_{fid} \\ r_{fid} = r_l \end{cases} \tag{122}$$

Where $i = 1, 2$ and (L_{xid}, L_{yid}) is the given parameter, representing the coordinate of the follower in the leader's body-fixed frame.

At this point, the control problem of the formation is transformed from "tracking the trajectory while maintain the formation shape" into the problem of "each follower tracking their own time-varying desired trajectory respectively".

For formation control, the controller designed in Chapter 4 is still used:

$$\tau_1 = \dot{u}_d + au_d + \frac{-r_d + \dot{\delta}}{c} v_d - \frac{f_1(\delta) + (1 - a\rho)u_e}{\rho} - k_u \tanh(z_1)$$

$$\tau_2 = -\kappa uv + \dot{r}_d - \ddot{\delta} + d\left(r_d - \dot{\delta}\right) - k_r \tanh\left(\bar{r}_e + \bar{\psi}_e\right)$$

Substituting (121) (122) into the expression of the controller, the follower controller can be expressed as follows:

$$\tau_{1,i} = \dot{u}_{fid} + au_{fid} + \frac{-r_{fid} + \dot{\delta}_{fi}}{c} v_{fid} - \frac{f_{fi1}(\delta) + (1 - a\rho)u_{fie}}{\rho} - k_{ui} \tanh(z_{fi1}) \tag{123}$$

$$\tau_{2,i} = -\kappa u_{fi} v_{fi} + \dot{r}_{fid} - \ddot{\delta}_{fi} + d\left(r_{fid} - \dot{\delta}_{fi}\right) - k_{ri} \tanh\left(\bar{r}_{fie} + \bar{\psi}_{fie}\right)$$

Where, δ_{fi} is defined by $\ddot{\delta}_{fi} + 2C_{\delta i}\dot{\delta}_{fi} + C_{\delta i}^2 \delta_{fi} = k_{fi} \tanh[(g_{fi} + u_{fid}) z_{fi2}] h_{fi}$; $u_{fie} = u_{fi} - u_{fid}$, $f_{1i}(\delta_i) = u_{fid}(1 - \cos\delta_{fi}) + v_{fid}\sin\delta_{fi}$;

$\dot{h}_{fi} = -k_{hi} r_{fid}^2 h_{fi},\ h_{fi}(0) = 1$, $\ddot{g}_{fi} = -k_{gi} u_{fid}^2 \dot{g}_{fi} - g_{fi},\ g_{fi}(0) = 1$

$z_{fi1} = x_{fie} + \rho u_{fie}$, $z_{fi2} = y_{fie} + \frac{\rho}{c} v_{fie}$, $\bar{\psi}_{fie} = \psi_{fi} - \psi_{fid} + \delta_{fi}$, $\bar{r}_{fie} = r_{fi} - r_{fid} + \dot{\delta}_{fi}$.

Because all the AUV models used in the formation are the same, the same values are used for the parameters $a,\ b,\ c,\ d,\ \rho$.

Since the controller structure is exactly the same as in Chapter 4, the control system stability and input saturation limits have been proved.

5.2.2. Simulation and analysis

In this thesis, the AUVs used in the formation are the same type, so the model parameters are the same as those in Chapter 4.

The model parameters of AUV are as follows:

$m_{11} = 120 \times 10^3 kg,\ m_{22} = 172.9 \times 10^3 kg,\ m_{33} = 636 \times 10^5 kg$
$d_{11} = 215 \times 10^2 kg \cdot s^{-1},\ d_{22} = 97 \times 10^3 kg \cdot s^{-1},\ d_{33} = 636 \times 10^5 kg \cdot s^{-1}$

Substitute the AUV physical model, the parameters of the system are

$a = 0.179,\ b = 0.561,\ c = 0.604,\ d = 0.126$
$\kappa = -8.32 \times e^{-4},\ \rho = c/b = 1.07665$

The initial state of the AUV is set to: $x_l(0) = 15m,\ y_l(0) = 15m,\ \psi_l(0) = 0.7rad$

$x_{f1}(0) = 10m,\ y_{fi}(0) = 10m,\ \psi_{fi}(0) = 0.7rad$, $x_{f2}(0) = 20m,\ y_{f2}(0) = 20m,\ \psi_{f2}(0) = 0.7rad$.

The maximum value of control input is set as $\bar{\tau}_{1,\max} = \bar{\tau}_{fi1,\max} = 6,\ \bar{\tau}_{2,\max} = \bar{\tau}_{fi2,\max} = 3$.

During tracking, the reference speed is set as $u_d = 1.0m/s,\ r_d = 0.02rad/s$.

In order to achieve better control performance, set the control parameters as:

$k_r = 0.5,\ k_u = 5,\ k_\delta = 1.8,\ C_\delta = 2,\ k_h = 50,\ k_g = 2$

$k_{ri} = 0.5,\ k_{ui} = 5,\ k_{\delta i} = 1.8,\ C_{\delta i} = 2,\ k_{hi} = 50,\ k_{gi} = 2$

Set the coordinate of the two followers in the leader's body-fixed frame respectively as: $L_{x1} = -5,\ L_{y1} = -5; L_{x2} = -5,\ L_{y2} = 5$.

In this thesis, 400s simulation time is set to simulate the trajectory tracking problem. The first 100s is linear trajectory tracking: $u_d = 1m/s,\ r_d = 0rad/s$, and the last 300s is curve trajectory tracking: $u_d = 1m/s,\ r_d = 0.02rad/s$.

The Simulink block diagram is as follows.

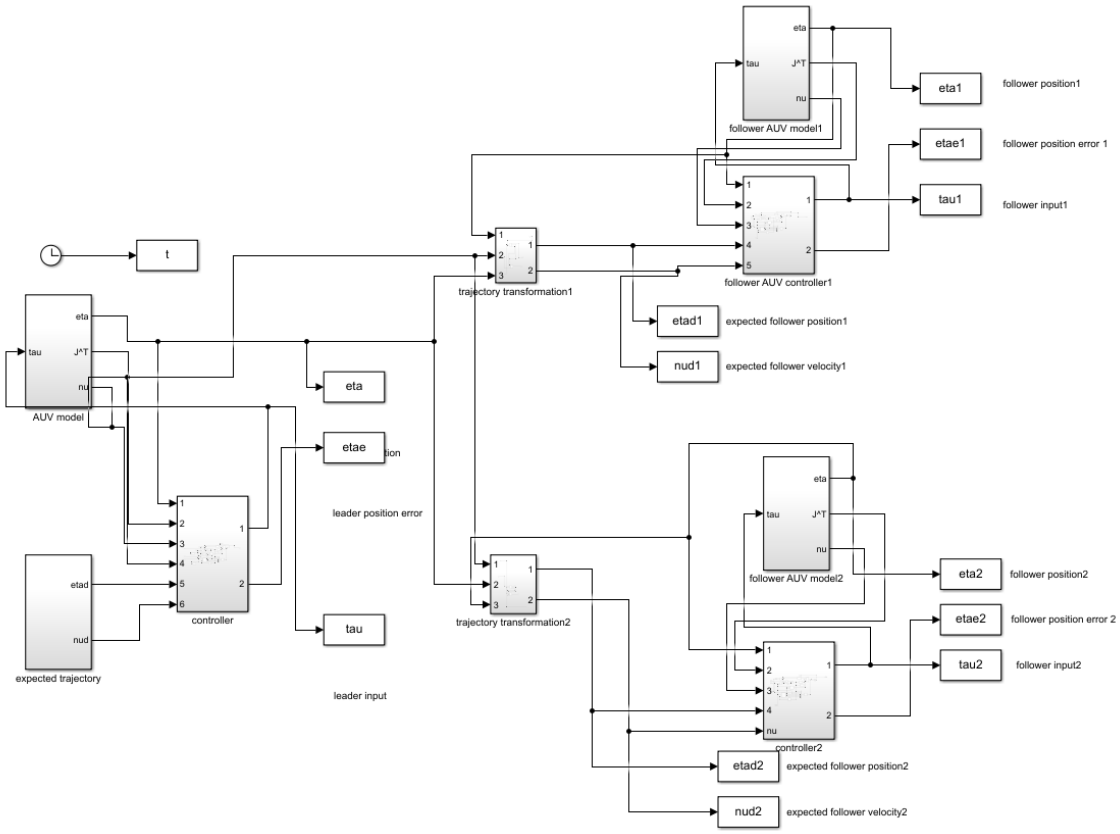

Figure 16. Simulink block diagram - AUV formation

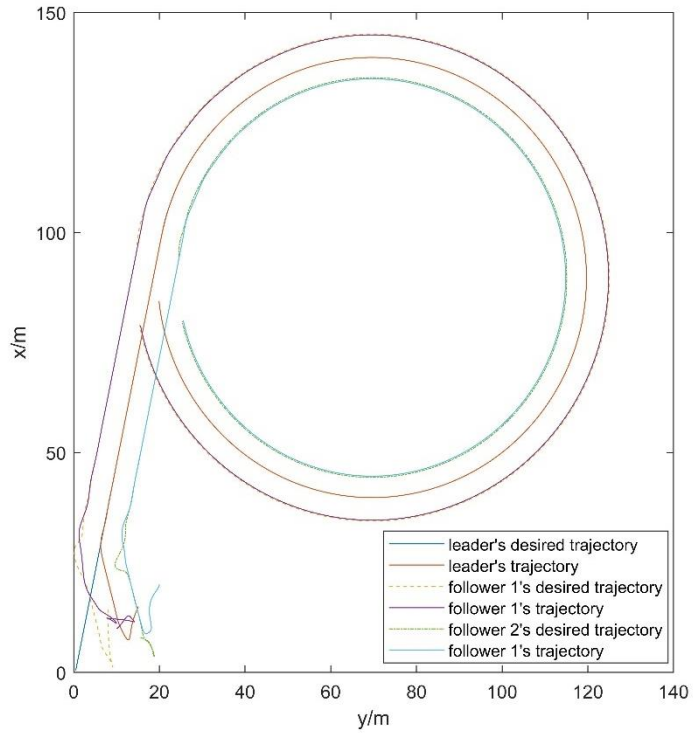

(a) trajectory tracking of AUV formation

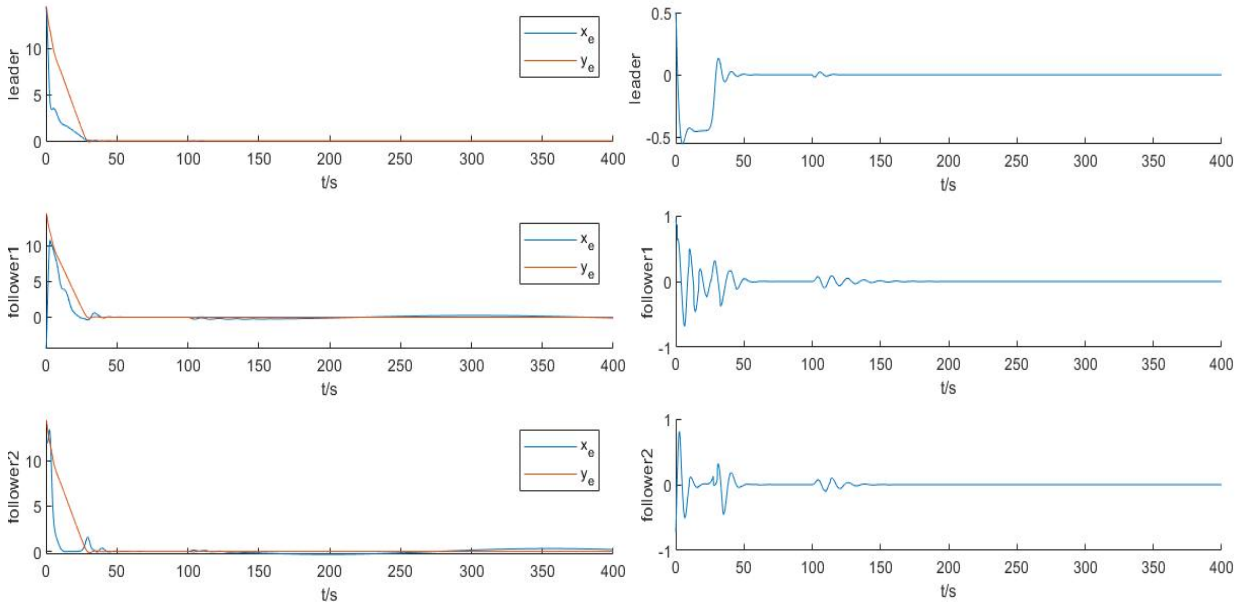

(b)tracking error of positon

(c)tracking error of angle

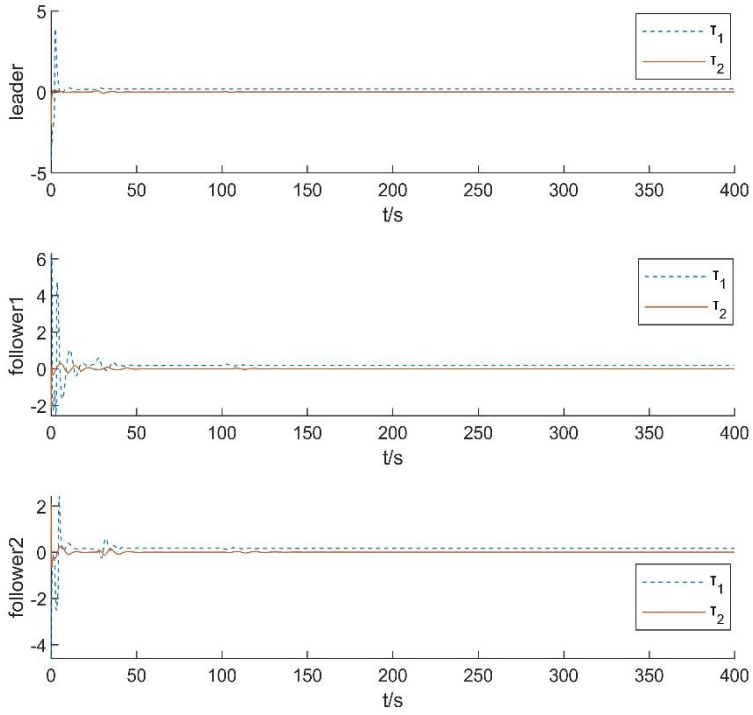

(d) Control inputs

Figure 17. Simulation results of AUV formation trajectory tracking

As shown in Figure 17, under the action of the controller designed in this thesis, The AUV formation can smoothly track the specified desired trajectory and keep the tracking error converging to a bounded small domain near the zero point. The control input does not exceed the maximum value the actuator can provide, and τ_2 gradually converges to the bounded small domain near the zero point over time.

Therefore, the control method proposed in this section can achieve the goal of tracking the desired trajectory and keep the formation during tracking.

5.3. Event trigger control for AUV formation tracking

5.3.1. Event triggers controller design

In this thesis, the leader's velocity will be used to design trigger conditions, and a joint trigger mechanism will be adopted, that is, as soon as any one of u_l, v_l, r_l meets its trigger conditions, the system will update the sampling.

Taking the event trigger of u_l as an example, the sampling error is defined as $\Delta_u = u_l(t) - \hat{u}_l(t)$, $i = 1, 2$, where $u_l(t)$ is the velocity of the leader at time t, and $\hat{u}_l(t)$ is the velocity signal that the leader sends to other followers.

Proportional threshold is adopted in this paper, and event-triggering condition is designed as the following form:

$$\begin{aligned} &\hat{u}_l(t) = u_l(t_{u,k}), \quad t \in [t_{u,k}, t_{u,k+1}) \\ &t_{u,k+1} = inf\{\Delta_u \geqslant A_u|\hat{u}_l| + B_u\} \end{aligned} \tag{124}$$

Where $k = 1, 2, 3\cdots$, $t_{u,0} = 0$, A_u, B_u are all suitable positive constants.

For v_l, r_l, the triggering condition has the same structure:

$$\begin{aligned} &\hat{v}_l(t) = v_l(t_{v,k}), \quad t \in [t_{v,k}, t_{v,k+1}) \\ &t_{v,k+1} = inf\{\Delta_v \geqslant A_v|\hat{v}_l| + B_v\} \end{aligned} \tag{125}$$

$$\begin{aligned} &\hat{r}_l(t) = r_l(t_{r,k}), \quad t \in [t_{r,k}, t_{r,k+1}) \\ &t_{r,k+1} = inf\{\Delta_r \geqslant A_r|\hat{r}_l| + B_r\} \end{aligned} \tag{126}$$

The working mechanism of trigger represented by Equation (124) is described as follows:

At trigger time $t_{u,k}$, the leader samples velocity signal $u_l(t)$: $\hat{u}_l(t) = u_l(t_{u,k})$, then use the signal transmitter to send it to the followers. This value keeps the same during the time period $t \in [t_{u,k}, t_{u,k+1})$. During this period followers will use a constant value $\hat{u}_l(t)$ to calculate their own desired velocity respectively. When sampling error Δ_u meet the trigger condition (124) again, the leader records the triggering time $t_{u,k+1}$, and carries on the sampling again for $u_l(t)$, and sends it to the followers. The value used by the followers to calculate their desired velocity is updated to $\hat{u}_l(t) = u_l(t_{u,k+1})$ and remains there until the next trigger time $t_{u,k+2}$...

The working mechanism of trigger with v_l, r_l as trigger condition is understood as above.

According to Formula (124), there exist function $\lambda_{u3}(t)$ and $\lambda_{u4}(t)$ which satisfy $|\lambda_{u3}(t)|, |\lambda_{u4}(t)| \leqslant 1$ and makes $u_l(t) = (1 + \lambda_{u3}(t) A_u)\hat{u}_l(t) + \lambda_{u4}(t) B_u$, that is:

$$\hat{u}_l = \frac{u_l - \lambda_{u4} B_u}{1 + \lambda_{u3} A_u} \tag{127}$$

The error between the actual velocity of the leader and the transmitted velocity signal is set to be:

$$u_{e,ETC} = u_l - \hat{u}_l = \frac{\lambda_{u3} A_u u_l + \lambda_{u4} B_u}{1 + \lambda_{u3} A_u} \tag{128}$$

According to the content in 4.3, u_l has a maximum value, so the velocity error $u_{e,ETC}$ can be controlled within a small acceptable magnitude by setting an appropriate coefficient $A_u,\ B_u$.

Similarly, the error $v_{e,ETC}$ and $r_{e,ETC}$ are bounded and controllable.

During formation operation, it is considered that the position and attitude of the leader can be obtained in real time by the sonar device of the follower without occupying communication resources.

5.3.2. Zeno Behavior Analysis

Write the motion equation of the leader according to Equation (40) :

$$\begin{cases} \dot{u}_l = \dfrac{1}{c} v_l r_l - a u_l + \tau_{l1} \\ \dot{v}_l = -c u_l r_l - b v_l \\ \dot{r}_l = k u_l v_l - d r_l + \tau_{l2} \end{cases} \tag{129}$$

It can be seen from the proof of saturation input of 4.3 that $u_l,\ v_l,\ r_l,\ \tau_{l1}, \tau_{l2}$ are both bounded. Observe equation (129) and it is easy to know that $\dot{u}_l,\ \dot{v}_l,\ \dot{r}_l$ have upper bounds, which can be denoted as $0 < \dot{u}_{l,\max},\ \dot{v}_{l,\max},\ \dot{r}_{l,\max} < +\infty$.

Taking the derivative of the sampling error $\Delta_u = u_l(t) - \hat{u}_l(t)$, $\hat{u}_l(t)$ does not change in the two nearest trigger intervals, so:

$$\dot{\Delta}_u = \dot{u}_l(t) \tag{130}$$

Considering that $\dot{u}_l(t)$ has a maximum value, then:

$$\left|\dot{\Delta}_u\right| = |\dot{u}_l| \leqslant u_{l,\max} \tag{131}$$

According to formula (124),

$$\begin{aligned} &\lim_{t \to t_{u,k}} |\Delta_u| = 0 \\ &\lim_{t \to t_{u,k+1}^-} |\Delta_u| = A_u |\hat{u}_l(t)| + B_u \end{aligned} \tag{132}$$

Combining equation (106) and (107), it can be seen that the lower bound of triggering interval $\Delta T_u = t_{u,k+1}^- - t_{u,k}$ must be satisfied:

$$inf(\Delta T_u)\dot{u}_{l,\max} \geqslant \min\{|\Delta_u|\} \tag{133}$$

Which means

$$\Delta T_u \geqslant \frac{A_u|u_l(t)|+B_u}{\dot{u}_{l,\max}} > 0 \tag{134}$$

Similarly, it is easy to prove that: $\Delta T_v \geqslant \frac{A_v|v_l(t)|+B_v}{\dot{v}_{l,\max}} > 0$, $\Delta T_r \geqslant \frac{A_r|r_l(t)|+B_r}{\dot{r}_{l,\max}} > 0$.

Let $\Delta T_{\mathrm{m}} = \min\{\Delta T_u, \Delta T_v, \Delta T_r\}$, according to the above analysis,

$$\Delta T > 0 \tag{135}$$

Thus, it can be proved that the minimum triggering interval of the ETC designed in this thesis must be positive, thus proving that Zeno phenomenon will not occur.

5.3.3. ETC simulation and analysis

To simulate the trajectory tracking control problem, a 400s simulation time is set. The first 100s is linear trajectory tracking: $u_d = 1m/s,\ r_d = 0rad/s$, and the last 300s is curve trajectory tracking: $u_d = 1m/s,\ r_d = 0.02rad/s$.

AUV model parameters used in this section are the same as those in the previous section.

The parameters of the event trigger are designed as follows:

$A_u = 0.01,\ B_u = 0.005;\ A_v = 0.005,\ B_v = 0.005,\ A_r = 0.005,\ B_r = 0.005$

The Simulink block diagram is as follows.

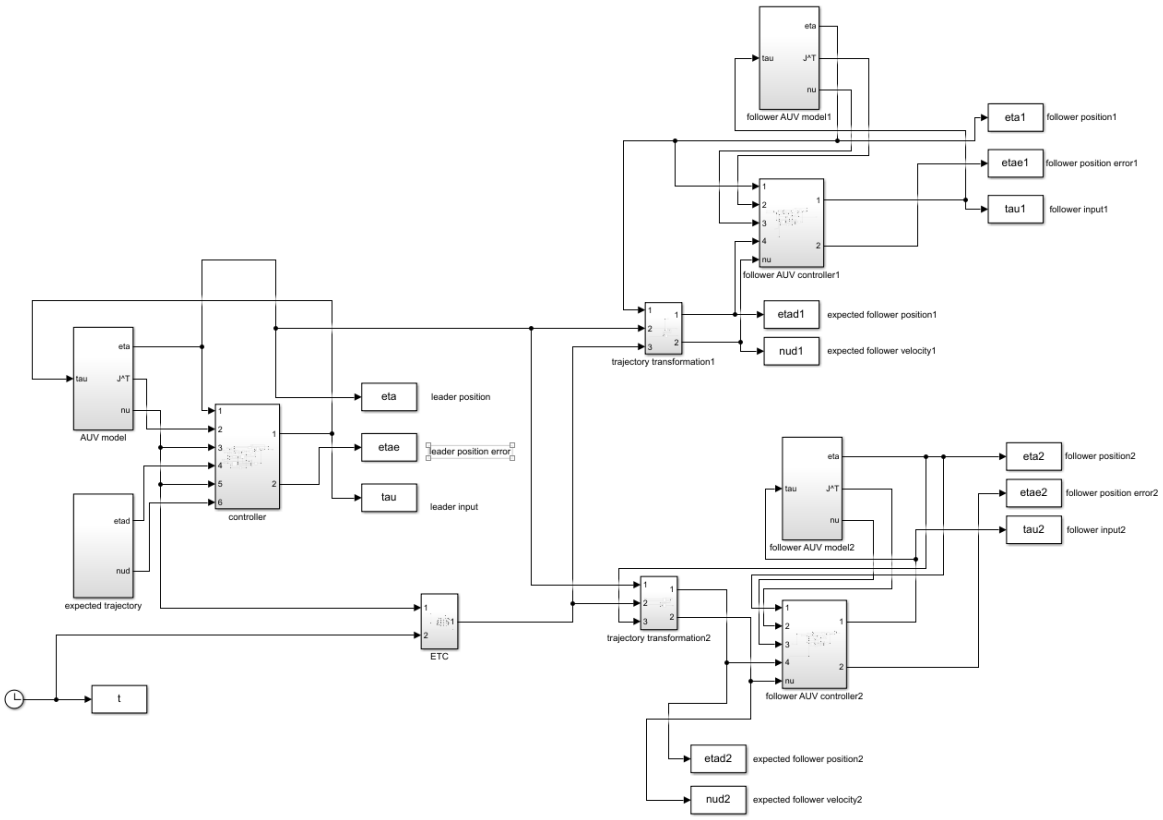

Figure 18. Simulink block diagram - AUV formation with ETC

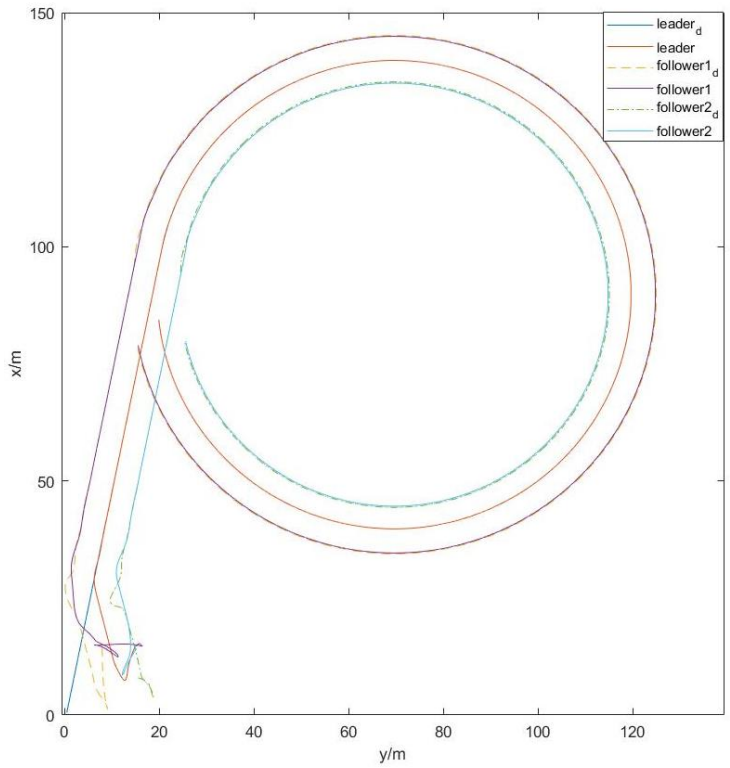

(a)ETC-based trajectory tracking of AUV formation

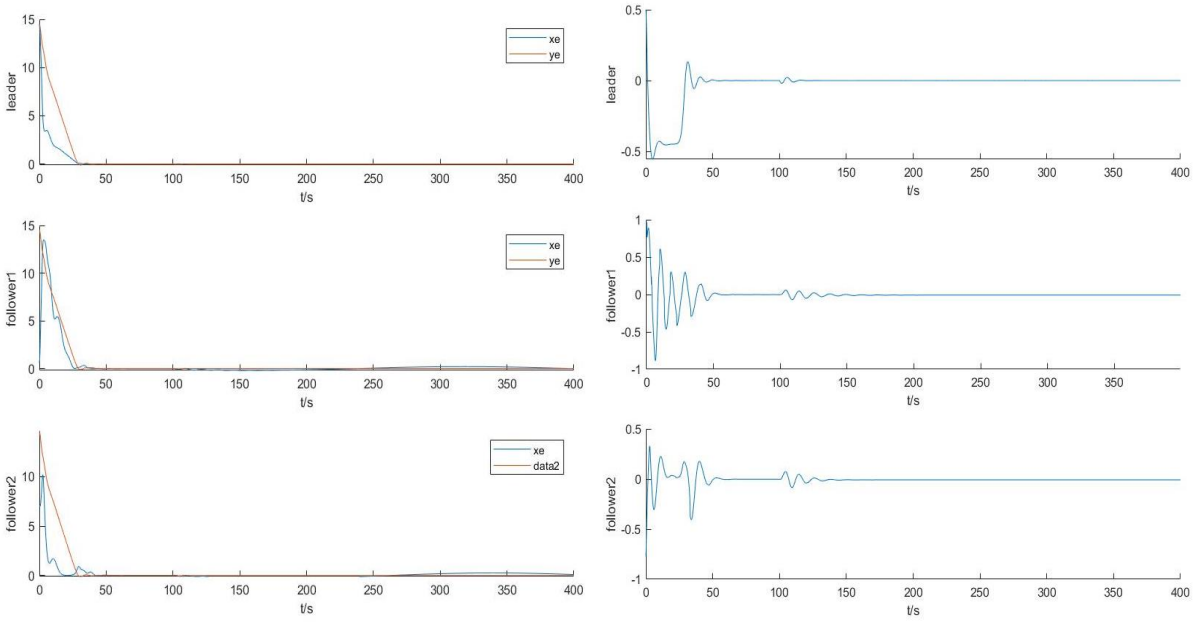

(b) Tracking error of position (c) Tracking error of angle

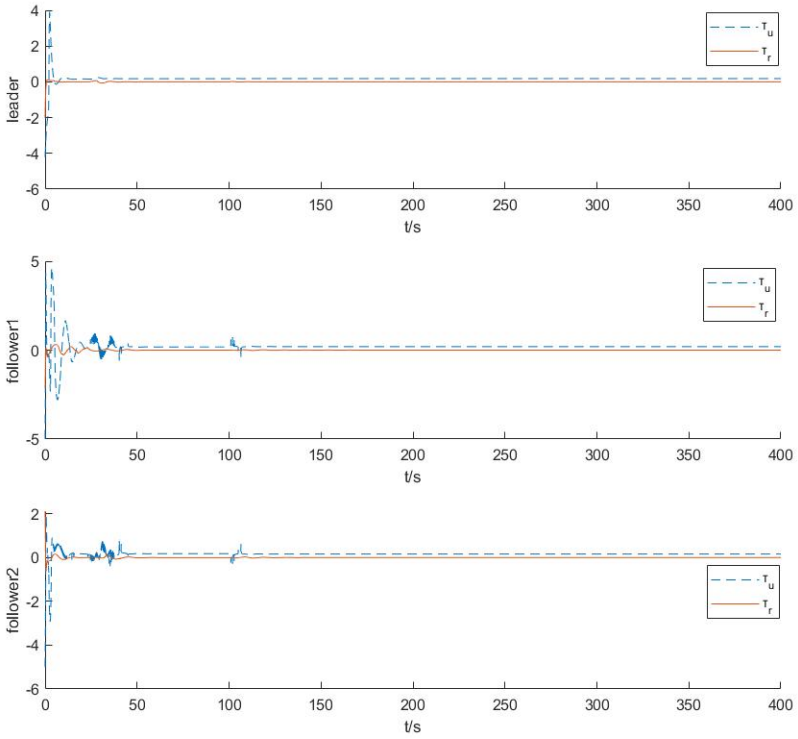

(d) Control inputs

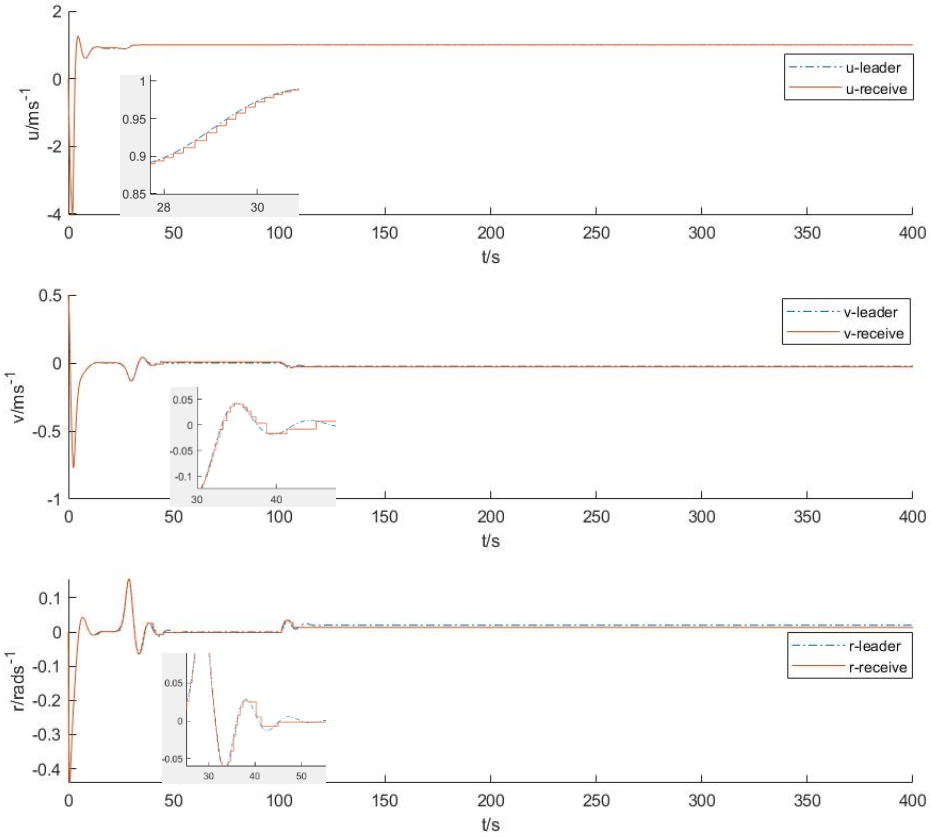

(e) Velocity of leader& velocity signal received by followers

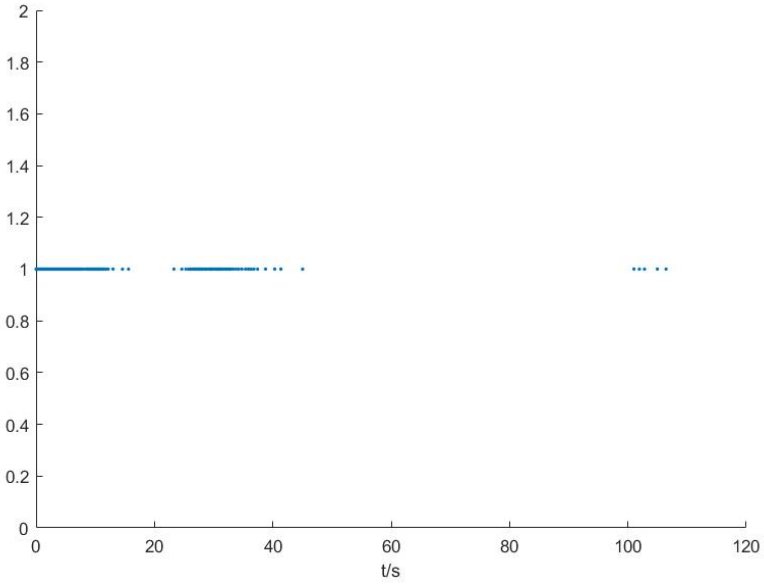

(f) Trigger time

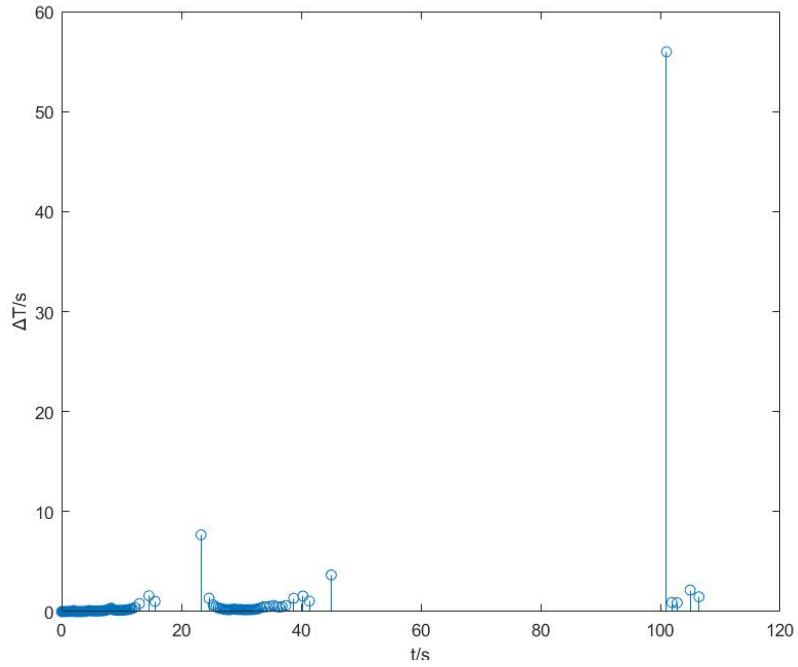

(g) Trigger span

Figure 19. Simulation of ETC-based trajectory tracking of AUV formation

As can be seen from Figure 19, in the process of formation trajectory tracking, the introduction of ETC has no obvious influence on the original control results and control efficiency.

The simulation results show that the formation can track the trajectory well, the tracking error converges to a bounded small region near zero, and the formation is maintained during the tracking process.

Simulation results show that the number of trigger sampling is 436 times, and the trigger frequency decreases significantly. After 107s, the trigger frequency even stops. Before that, the maximum trigger interval can reach 55.98s. In practice, it can greatly reduce the occupation of AUV communication resources and adapt to the communication restricted environment.

Chapter 6. Conclusion

6.1. Work in the thesis

In this thesis, different control methods and strategies are proposed for the simultaneous stabilization and tracking of a single underactuated AUV and the trajectory tracking of AUV formation in two-dimension.

First of all, this thesis introduces AUV and the necessity of AUV research, and then puts forward the goal: to effectively control a single underactuated AUV and underactuated AUV formation, and to reduce the frequency of AUV actuator use and the frequency of AUV formation communication through the strategy of event trigger control.

Then, the thesis introduces some basic knowledge needed to facilitate the subsequent completion of the thesis.

In this thesis, a controller which can control the AUV simultaneously to track trajectory and stabilize is proposed, so that it does not need to switch controllers when it is working. The second order differential small quantity is introduced in the design to avoid the phenomenon of too many parameters when using backstep method. At the same time, the controller can meet the requirements of saturation input. Considering that the actuator of AUV needs to receive and execute the time-varying input signal at any time, which will reduce the service life of the device, an event triggering mechanism is designed to adjust the execution input when the difference between the calculated input signal and the execution input signal reaches a certain magnitude.

MATLAB Simulink module is used to simulate the effect of simultaneous controller and the ETC respectively, simulation results both show good control effect. Especially, the effect of ETC to reduce the triggering times of actuators is obvious, which can prove that this design can reduce the frequency of actuator adjustment, prolong the service life of equipment, with both reliability and economy.

Finally, combined with the idea of light-of-sight method and virtual structure method, the 2-dimensional horizontal AUV formation tracking control problem is transformed into the problem that followers tracking their respective desired trajectory, and the control is carried out on the basis of the controller in Chapter 4.

For deep sea conditions, communication resource is extremely limited. An event trigger mechanism is designed, which makes the AUVs communicate discontinuously with the triggering condition. When the change of leader's velocity achieves a certain condition, the velocity information is sent to the followers through communication equipment, which reduce the frequency of communication.

At last, the formation control method is simulated by MATLAB Simulink. It can be seen from the simulation results that the control method proposed in this chapter is effective for formation control, and the addition of trigger makes AUV transmit individual state information only when it is necessary, which basically has no influence on formation tracking effect. In this way, communication resources are saved and reliability and economy are balanced.

6.2. Future work

There are two main lines in which this work may be improved in the future:

(1) The controller of a single AUV can satisfy simultaneous tracking and stabilization, but the chattering in the stabilization process is obvious, and further improvements to make the control convergence effect smoother could be considered;

(2) The line-of-sight method is an estimation method. Combined with the virtual structure method, the conversion of the follower's expected trajectory is not suitable for the stabilization of the AUV formation. A more suitable method can be considered to obtain the followers' expected trajectory, so as to achieve the purpose of simultaneous tracking and stabilizing of AUV formations.

Bibliography and references

[1] Samson, C. (2002). Control of chained systems application to path following and time-varying point-stabilization of mobile robots. IEEE Transactions on Automatic Control, 40(1), 64-77.

[2] Lapierre, L. & Jouvencel, B. (2007). Nonlinear path following control of an auv. Ocean Engineering, 34(2), 1734-1744.

[3] Yu, D., Xia, Y., Li, L., & Zhai, D. H. (2020). Event-triggered distributed state estimation over wireless sensor networks. Automatica, 118, 109039.

[4] SNAME, The Society of Naval Architects and Marine Engineers. (1950). Nomenclature for treating the motion of a submerged body through a fluid. T & R Bulletin.

[5] K. D. Do., Z. P. Jiang, & J. Pan. (2002). Universal controllers for stabilization and tracking of underactuated ships. Systems & Control Letters, 47(4), 299-317.

[6] Khodayari, M. H., & Balochian, S. (2015). Modeling and control of autonomous underwater vehicle (auv) in heading and depth attitude via self-adaptive fuzzy pid controller. Journal of Marine Science and Technology, 20(3), 559-578.

[7] Yang, J., Jie, W. U., & Yue, H. U. (2002). Backstepping method and its applications to nonlinear robust control. Control & Decision (Suppl), 641-647.

[8] Li, J. H., & Lee, P. M. (2005). Design of an adaptive nonlinear controller for depth control of an autonomous underwater vehicle. Ocean Engineering, 32(17–18), 2165-2181.

[9] Liu J. K., Sun F. C.. (2007). Research and development on theory and algorithms of sliding mode control, 24(3), 407-418.

[10] Akkizidis, I. S., & Roberts, G. N. (1998). Fuzzy modelling and fuzzy-neuro motion control of an autonomous underwater robot. International Workshop on Advanced Motion Control. IEEE.

[11] Hunt, K. J., Sbarbaro, D., Zbikowski, R., & Gawthrop, P. J. (1992). Neural networks for control systems—a survey. Automatica, 28(6), 1083-1112.

[12] K. D. Do, Z. P. Jiang & B, J. Pan (2002). Universal controllers for stabilization and tracking of underactuated ships. Systems & Control Letters, 47(4), 299-317.

[13] Fan, Y., Feng, G., Wang, Y., & Song, C. (2013). Distributed event-triggered control of multi-agent systems with combinational measurements. Automatica, 49(2), 671-675.

[14] Borhaug, E., Pavlov, A., & Pettersen, K. Y. (2008). Integral LOS control for path following of underactuated marine surface vessels in the presence of constant ocean currents. IEEE Conference on Decision & Control. IEEE.

[15]https://www.worldatlas.com/r/w960-q80/upload/fb/bb/c2/shutterstock-1260577537.jpg (2021)

-[16]http://geo-marine-tech.com.cn/UpLoadFile/20150703/f61eb01d-8257-4e82-b6b7-a4eb338a4ea2.jpg (2019)

[17] Xu, H., Zhang, G. C., Sun, Y. S., Pang, S. & Wang, X. B. (2019). Design and experiment of a plateau data-gathering AUV. Journal of Marine Science and Engineering, 7(10), 376.[18]http://mms1.baidu.com/it/u=3252078766,391018478&fm=253&app=138&f=JPEG&fmt=auto&q=75?w=640&h=427 (2017)

[19] Birk, A., Pascoal, A., Antonelli, G., Caiti, A., Casalino, G. & Indiveri, G., et al. (2012). Cooperative cognitive control for autonomous underwater vehicles (CO3AUVs): overview and progresses in the 3rd project year. Ifac Proceedings Volumes, 45(5), 361-366.

[20] Zhou, J. W. (2019). Three-dimensional path tracking control of underactuated AUVs with input saturation. Nibo University (Doctoral dissertation).